

# A Nuclear Magnetic Resonance Spectroscopic Technique for the Characterization of Lithium Ion Pair Structures in THF and THF/HMPA Solution<sup>1</sup>

Hans J. Reich,\* Joseph P. Borst, Robert R. Dykstra, and D. Patrick Green

Contribution from the Department of Chemistry, University of Wisconsin, Madison, Wisconsin 53706

Received April 1, 1993

**Abstract:** Lithium cations coordinated by HMPA undergo sufficiently slow dynamic exchange on the NMR time scale at low temperature that distinct cation–HMPA complexes can usually be observed. This observation is the basis for a new technique to quickly and unambiguously determine the ion pair structure of lithium reagents in THF and THF/HMPA solution using low-temperature <sup>7</sup>Li and <sup>31</sup>P NMR. In this paper we describe the procedures for assigning structures to HMPA-complexed separated and contact lithium cations. The application of this technique to ion pair structure determination of several lithium reagents is also presented. The HMPA titrations of fluorenyllithium, trityllithium, and lithium triphenylmercurate (Ph<sub>3</sub>HgLi) in THF solution give similar results. All are solvent-separated ion pairs in THF. The progressive coordination of four HMPA molecules to the lithium cation can be observed in the <sup>7</sup>Li and <sup>31</sup>P NMR through characteristic chemical shifts and <sup>2</sup>J<sub>Li-P</sub> scalar coupling. Under the same conditions LiI, LiBr, and MeSeLi are contact ion pairs and become almost completely solvent-separated upon addition of 3 equiv of HMPA. Our results show that MeSLi and LiCl are aggregated in THF, and the addition of HMPA not only breaks down the dimers to monomers but also causes ion separation on addition of 6 equiv of HMPA. Phenyllithium can be deaggregated from dimer to monomer, but even a high concentration of HMPA fails to cause significant ion pair separation. The tetrameric methyllithium, on the other hand, undergoes no visible dissociation to dimers and monomers on addition of HMPA; only coordination of the four corners of the methyllithium tetrahedron with HMPA is observed.

Understanding the solution structure of lithium reagents is important for effectively rationalizing and predicting their reactivity and/or selectivity. In nonpolar and weakly polar solvents (hydrocarbons, diethyl ether) *aggregation phenomena* play an important role in determining reactivity. However, in the more polar media commonly used (THF and mixtures of it with more strongly coordinating solvents), many organolithium reagents, particularly those with one or two carbanion stabilizing groups, have become largely deaggregated.<sup>2</sup> Under these conditions reactivity is dominated by details of *ion pair structure*. By this we mean the coordination of lithium by the solvent or solvent additives and the contact or solvent-separated ion pair dichotomy (CIP/SIP). In particular, strongly coordinating ligands will weaken coordination between lithium and the counterion and increase the anionic reactivity of the counterion.<sup>3</sup> Eventually a solvent-separated ion pair forms with greatly increased<sup>4a</sup> or substantially modified<sup>4b</sup> reactivity.

Reich, Green, and Phillips,<sup>1a,b</sup> in connection with NMR studies of the metal–halogen exchange,<sup>1c,d</sup> and independently Snaith and co-workers,<sup>5</sup> as part of their extensive series of crystal structures of HMPA complexes, reported the first lithium–phosphorus (<sup>2</sup>J<sub>Li-P</sub>) coupling for an HMPA-complexed lithium cation in THF. This observation provides valuable direct evidence for solution structures of organolithium species since it enables determination of the number of HMPA molecules attached to lithium. Recently we have reported the application of this NMR spectroscopic technique to carbanions which are solvent-separated and contact ion pairs in THF and have identified the ion separation process for 2-lithio-2-(phenyldimethylsilyl)-1,3-dithiane.<sup>1e</sup> The technique has also been used to study solvation and reactivity of lithium amides<sup>6</sup> and lithium phenoxides.<sup>7</sup> This paper expands on the procedures we use for making assignments of structure to HMPA-complexed contact and separated lithium cations and applies the technique to several lithium reagents.

The observation of slow exchange on the NMR time scale between HMPA and its complexes with metal ions,<sup>8</sup> as well as *J*-coupling between the phosphorus of HMPA and a coordinated metal ion, is precedented<sup>9</sup> and has been used to provide structural and mechanistic information about metals more Lewis acidic than lithium, such as aluminum and zinc. The present study explores the coordination chemistry of HMPA and lithium cations in a variety of compounds.

(1) (a) Reich, H. J.; Green, D. P.; Phillips, N. H. *J. Am. Chem. Soc.* **1989**, *111*, 3444. (b) Reich, H. J.; Green, D. P. *J. Am. Chem. Soc.* **1989**, *111*, 8729. (c) Reich, H. J.; Green, D. P.; Phillips, N. H. *J. Am. Chem. Soc.* **1991**, *113*, 1414. (d) Green, D. P. Ph.D. Dissertation, University of Wisconsin—Madison, 1989. (e) Reich, H. J.; Borst, J. P. *J. Am. Chem. Soc.* **1991**, *113*, 1835. Reich, H. J.; Dykstra, R. R. *J. Am. Chem. Soc.* **1993**, *115*, 7041. (f) Dykstra, R. R.; Reich, H. J. Unpublished results. (g) Reich, H. J.; Green, D. P.; Phillips, N. H.; Borst, J. P. *Phosphorus Sulfur* **1992**, *67*, 63. (h) Reich, H. J.; Gudmundsson, B. Ó.; Dykstra, R. R. *J. Am. Chem. Soc.* **1992**, *114*, 7937. (i) Reich, H. J.; Phillips, N. H. *J. Am. Chem. Soc.* **1986**, *108*, 2102.

(2) The following lithium reagents are partially or completely monomeric in THF: phenyllithium,<sup>1a,c,2a</sup> *sec*-butyllithium,<sup>2a</sup> *tert*-butyllithium,<sup>2a</sup> (phenyldimethylsilyl)lithium,<sup>2b</sup> (diphenylphosphinomethyl)lithium,<sup>2c</sup> and 7-norbornadienyllithium.<sup>2d</sup> (a) Bauer, W.; Winchester, W. R.; Schleyer, P. v. R. *Organometallics* **1987**, *6*, 2371. (b) Edlund, U.; Lejon, T.; Venkatachalam, T. K.; Bunzel, E. *J. Am. Chem. Soc.* **1985**, *107*, 6408. (c) Fraenkel, G.; Winchester, W. R.; Williard, P. G. *Organometallics* **1989**, *8*, 2308. (d) Goldstein, M. J.; Wenzel, T. T. *Helv. Chim. Acta* **1984**, *67*, 2029.

(3) Bartlett, P. D.; Goebel, C. V.; Weber, W. P. *J. Am. Chem. Soc.* **1969**, *91*, 7425.

(4) (a) Hogen-Esch, T. E. *Adv. Phys. Org. Chem.* **1977**, *15*, 153. (b) Cohen, T.; Abraham, W. D.; Myers, M. *J. Am. Chem. Soc.* **1987**, *109*, 7923. Brown, C. A.; Yamaichi, A. *J. Chem. Soc., Chem. Commun.* **1979**, 100.

(5) (a) Barr, D.; Doyle, M. J.; Mulvey, R. E.; Raithby, P. R.; Berd, D.; Snaith, R.; Wright, D. S. *J. Chem. Soc., Chem. Commun.* **1989**, 318. (b) Raithby, P. R.; Reed, D.; Snaith, R.; Wright, D. S. *Angew. Chem., Int. Ed. Engl.* **1991**, *30*, 1011. (c) Barr, D.; Clegg, W.; Mulvey, R. E.; Snaith, R. *J. Chem. Soc., Chem. Commun.* **1984**, 79.

(6) Romesberg, F. E.; Gilchrist, J. H.; Harrison, A. T.; Fuller, D. J.; Collum, D. B. *J. Am. Chem. Soc.* **1991**, *113*, 5751. Romesberg, F. E.; Collum, D. B. *J. Am. Chem. Soc.* **1992**, *114*, 2112.

(7) Jackman, L. M.; Chen, X. *J. Am. Chem. Soc.* **1992**, *114*, 403.

(8) Tkaczuk, M. N.; Lincoln, S. F. *Aust. J. Chem.* **1980**, *33*, 2621.

(9) Delpuech, J.-J.; Khaddar, M. R.; Peguy, A. A.; Rubini, P. R. *J. Am. Chem. Soc.* **1975**, *97*, 3373. Wharf, I.; Onyszchuk, M. *J. Organomet. Chem.* **1980**, *190*, 417.

## Introduction

Positive evidence for the solution ion pair structure (as well as degree of aggregation) of lithium compounds which are contact ions can sometimes be established from the observation of one-bond  $J$ -coupling between lithium and adjacent nuclei such as  $^{13}\text{C}$ ,  $^{29}\text{Si}$ ,  $^{31}\text{P}$ ,  $^{12}\text{C}$ ,  $^{29}\text{Si}$ ,  $^{77}\text{Se}$ ,  $^{19}\text{F}$  or  $^{119}\text{Sn}$ .<sup>1f,13</sup> The inability to observe coupling is less informative since effects other than ion separation could be responsible. For example,  $J$  could be too small to detect, or coupling could be averaged by fast exchange or quadrupolar relaxation. Furthermore, when the nucleus does not have an effective NMR isotope (e.g., S, O, Cl, Br, I), coupling cannot be used. Detailed NMR and UV spectroscopic studies combined with colligative property measurements have provided much information on ion pair status.<sup>14</sup> The interpretation of such data is difficult because no direct information on the actual solvation status of the lithium cation is obtained, but instead, reliance is made on a physical property (e.g.,  $^1\text{H}$  or  $^{13}\text{C}$  chemical shift or UV absorption) which changes in some systematic but not entirely predictable way as solvent, temperature, and cation are changed.

The technique that we have developed allows us to obtain detailed information on solution ion pair structure with much less experimental effort, and for anions which have no usable UV or NMR properties themselves. To firmly establish the applicability of our new technique, we felt it was crucial to determine whether the NMR properties ( $^7\text{Li}$  and  $^{31}\text{P}$  chemical shifts and coupling constants) of various  $\text{Li}h_n^+$  species during an HMPA titration could be used to unambiguously determine the structure of separated and contact ions. We will abbreviate  $[\text{Li}(\text{HMPA})_n(\text{THF})_m]^+$  as  $\text{Li}h_n^+$  where  $n = 0-4$ , and  $m =$  an unknown number of solvent molecules needed to satisfy the solvation requirements of a particular lithium cation. When referred to specifically, contact ions will be represented as  $\text{R}-\text{Li}h_n$  and solvent-separated ions as  $\text{R}-//\text{Li}h_n^+$  where the symbol  $//$  indicates at least one layer of solvent between the anion and the cation.

## Results and Discussion

**The HMPA Titration Technique.** The procedures we have used in this study require no special equipment other than a modern multinuclear NMR spectrometer capable of very low temperature operation. We carry out an HMPA titration of a lithium reagent (typically at  $\approx 0.15$  M concentration) and follow developments by  $^7\text{Li}$  (or  $^6\text{Li}$ ) and  $^{31}\text{P}$  NMR and where appropriate by using other nuclei as well. Temperatures below  $-110$  °C are essential for observing Li-P coupling, and it is principally the multiplicity, together with line width and chemical shift of the lithium signals, which allows us to establish at an unprecedented level of detail solution ion pair structures and solvation of lithium.

In the following sections we first discuss some technical aspects of the HMPA titration experiment. We then perform a detailed NMR study of the model separated ion pair fluorenyllithium, including temperature and concentration dependence, a solvent effect, and the effect of another potential donor/acceptor ligand, diisopropylamine. We then examine a series of lithium reagents: first, several separated ion pairs; then contact ion pairs, starting

(10) Fraenkel, G.; Fraenkel, A. M.; Geckle, M. J.; Schloss, F. J. *Am. Chem. Soc.* **1979**, *101*, 4745. Fraenkel, G.; Pramanik, P. *J. Chem. Soc., Chem. Commun.* **1983**, 1527.

(11) (a) Seebach, D.; Siegel, H.; Gabriel, J.; Hässig, R. *Helv. Chim. Acta* **1980**, *63*, 2046. (b) Seebach, D.; Hässig, R.; Gabriel, J. *Helv. Chim. Acta* **1983**, *66*, 308.

(12) Colquhoun, I. J.; McFarlane, H. C. E.; McFarlane, W. J. *Chem. Soc., Chem. Commun.* **1982**, 220.

(13) Reed, D.; Stalke, D.; Wright, D. S. *Angew. Chem., Int. Ed. Engl.* **1991**, *30*, 1459.

(14) (a) Hogen-Esch, T. E.; Smid, J. *J. Am. Chem. Soc.* **1966**, *88*, 307. (b) Hogen-Esch, T. E.; Smid, J. *J. Am. Chem. Soc.* **1966**, *88*, 318. (c) Smid, J. *Ions and Ion Pairs in Organic Reactions*; Szwarc, M., Ed.; Wiley-Interscience: New York, 1972; Vol. I, pp 85-151. (d) O'Brien, D. H.; Russell, C. R.; Hart, A. J. *J. Am. Chem. Soc.* **1979**, *101*, 633. (e) Grutzner, J. B.; Lawlor, J. M.; Jackman, L. M. *J. Am. Chem. Soc.* **1972**, *94*, 2306. (f) Gronert, S.; Streitwieser, A., Jr. *J. Am. Chem. Soc.* **1988**, *110*, 2836.

with the readily separable lithium iodide and proceeding to the inseparable phenyllithium and methyllithium.

**The Lithium Isotopes.** We have found that the easily observed and sensitive  $^7\text{Li}$  at natural abundance (95%,  $I = 3/2$ ) serves well in most cases, as illustrated in the spectra presented in this paper. In some situations the use of  $^6\text{Li}$  (5%,  $I = 1$ ) provides advantages, as has been well demonstrated by Fraenkel and others.<sup>10</sup> There are two main sources of broadening in lithium NMR spectra: dynamic exchange ( $T_2$ ) and quadrupolar relaxation ( $T_1$ ). Since the interactions we are studying are weak, we routinely operate at the low-temperature limits of the solvent system and spectrometer to minimize dynamic exchange. Even at the lowest accessible temperatures ( $\approx -145$  °C), some contact ions are still subject to  $T_2$  broadening. For such systems,  $^7\text{Li}$  is the isotope of choice because the Li-P coupling constants of  $^7\text{Li}$  are larger by a factor of 2.64 ( $\gamma(^7\text{Li})/\gamma(^6\text{Li})$ ), and signals are separated by chemical shifts (in hertz) that are larger by the same factor. Hence, closely spaced peaks (whether due to  $J$  or  $\delta$ ) can be distinguished under conditions of faster dynamic exchange. For some contact ions the quadrupolar ( $T_1$ ) broadening of  $^7\text{Li}$  makes it advantageous to use  $^6\text{Li}$ , which will have much longer  $T_1$  values and sharper lines. Occasionally, ions coordinated to one or two HMPAs may be both  $T_1$  and  $T_2$  broadened, and neither isotope can provide cleanly resolved multiplets. We first run  $^7\text{Li}$ , and if necessary, enriched or natural abundance  $^6\text{Li}$ .

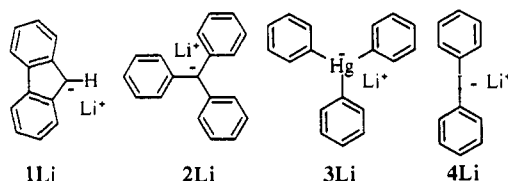
The smaller  $^2J_{\text{Li-P}}$  coupling of  $^6\text{Li}$  has one very great advantage in the  $^{31}\text{P}$  spectra: the width of the 1:1:1 triplets of  $^6\text{Li}$ -coupled signals is only 1/4 that of  $^7\text{Li}$  1:1:1 quartets ( $J$  is 0.38 as large, and the multiplet is only  $2J$  wide, rather than  $3J$ ). This gives much improved dispersion in the  $^{31}\text{P}$  NMR spectra, resulting in better detection of multiple ions in complex solutions and more accurate quantification of ion concentrations.

**Temperatures and Solvents.** This paper deals principally with experiments in THF, which is the most important solvent in organolithium chemistry. Although the freezing point of THF is  $-108$  °C, we can routinely supercool solutions to  $-120$  °C for measurement of  $^{31}\text{P}$ ,  $^7\text{Li}$ , or enriched  $^6\text{Li}$  spectra which typically require less than 10 min. When less sensitive nuclei such as natural abundance  $^6\text{Li}$ ,  $^{13}\text{C}$ ,  $^{29}\text{Si}$ , or  $^{77}\text{Se}$  are being observed, the typical time to obtain a spectrum on a 0.15 M solution increases to 30-60 min, and it is difficult to avoid freezing of the sample. We, therefore, routinely use 60:40 THF/ether mixtures, which work well to  $-135$  °C. The behavior of ions in this mixture is only marginally different than in pure THF. Dimethyl ether is more cumbersome to use as an additive, but it allows lower temperatures (down to  $-150$  °C) and it is closer in polarity to THF than is diethyl ether. See Figure 18 for an example.

The use of pure ether as solvent for HMPA titrations is limited by the difficulty of preparing many lithium reagents in ether, and by the poor solubility of many  $\text{LiX}$  species and their HMPA solvates at the low temperatures of our experiment.

## Solvent-Separated Ions

We began our study by comparing a series of lithium species which are known to be, or can reasonably be expected to be, separated ions in THF and whose HMPA complexes should also be separated. These include fluorenyllithium (1Li), trityllithium (2Li), and the "ate" complexes 3Li and 4Li.



**Fluorenyllithium.** The favorable UV properties, ease of preparation, and stability of fluorenyllithium alkali metal salts have

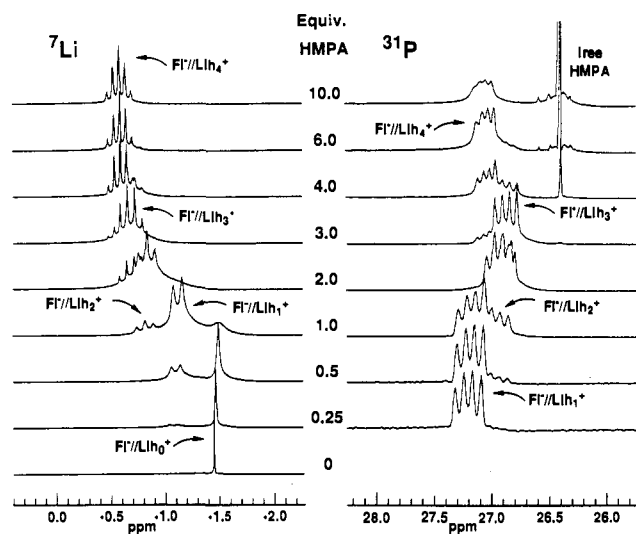


**Figure 1.** HMPA titration of 0.16 M fluorenyllithium (1Li) in 20:1 THF/hexane at  $-125\text{ }^{\circ}\text{C}$ . Spectra are plotted at the same frequency scale.

made them among the most studied of all carbanions.<sup>14</sup> Hogen-Esch<sup>14a</sup> and Smid,<sup>14b</sup> who investigated lithium fluorenyl by UV-visible spectroscopy and conductivity studies, found that fluorenyllithium is about 80% dissociated at  $25\text{ }^{\circ}\text{C}$  in THF. Using  $^{13}\text{C}$  NMR spectroscopy, O'Brien et al.<sup>14c</sup> measured equilibrium constants at different temperatures in THF and reported that fluorenyllithium is greater than 91% separated at  $-25\text{ }^{\circ}\text{C}$ . Lower temperatures favor separated ions over contact ions (ion separation is enthalpically favored), so fluorenyllithium must be essentially fully separated at the low temperatures of our experiment. Other researchers have used NMR spectroscopy in their studies of lithium fluorenyl: Jackman et al. ( $^1\text{H}$  NMR),<sup>14d</sup> Schleyer et al. ( $^6\text{Li}$ ,  $^1\text{H}$  heteronuclear Overhauser effect spectroscopy, HOESY),<sup>15</sup> and most recently Edlund et al. ( $T_{1\rho}$  and  $T_1$  studies).<sup>16</sup>

The HMPA titration for fluorenyllithium is shown in Figure 1. Except when noted, the  $^7\text{Li}$  and  $^{31}\text{P}$  spectra are plotted at the same frequency scale. The first aspect to note is that the  $^7\text{Li}$  singlet at 0 equiv of HMPA is very sharp ( $\nu_{1/2} = 1.1\text{ Hz}$ ), a characteristic of a tetrahedrally solvated, solvent-separated  $^7\text{Li}$  cation. The addition of HMPA to the solution caused the appearance of a new signal, a doublet due to a  $^2J_{\text{Li-P}}$  coupling of one HMPA  $^{31}\text{P}$  (spin =  $1/2$ ) to  $^7\text{Li}$  (spin =  $3/2$ ). The singlet and doublet are broadened due to dynamic exchange. As more HMPA was added, other separated species were observed: a triplet ( $\text{LiH}_2^+$ ), a quartet ( $\text{LiH}_3^+$ ), and a quintet ( $\text{LiH}_4^+$ ). The order of  $\delta$  values for the different complexes is  $\text{LiH}_1^+ < \text{LiH}_2^+ < \text{LiH}_3^+ < \text{LiH}_4^+$  for all separated ions studied.

One remarkable aspect of this series of spectra is the downfield movement of the  $^7\text{Li}$  signal as the  $\text{LiH}_1^+$ ,  $\text{LiH}_2^+$ ,  $\text{LiH}_3^+$ , and  $\text{LiH}_4^+$  species are formed. It seems likely that the principal cause of the lithium NMR shifts is changes in the average distance of lithium from fluorenyl. In fact, the  $\text{LiH}_4^+$  ( $-0.51 \pm 0.05$ ) and  $\text{LiH}_3^+$  ( $-0.61 \pm 0.05$ ) chemical shifts are nearly identical to those of all other separated ions examined, and these ions should have the greatest anion-cation separation. The shifts of  $\text{LiH}_2^+$ ,  $\text{LiH}_1^+$ , and  $\text{LiH}_0^+$  are progressively more upfield as the average position of the lithium cation approaches the strongly shielding region above the fluorenyl ring. Such upfield shifts were not observed for less magnetically active counterions such as  $\text{PhBET}_3^-$  or  $\text{Ph}_3\text{C}^-$ . Note, however, that the total range of these shifts ( $\sim 1\text{ ppm}$ ) is still small compared to the chemical shift of the contact ion ( $\Delta\delta > 4.5\text{ ppm}$ , see below).

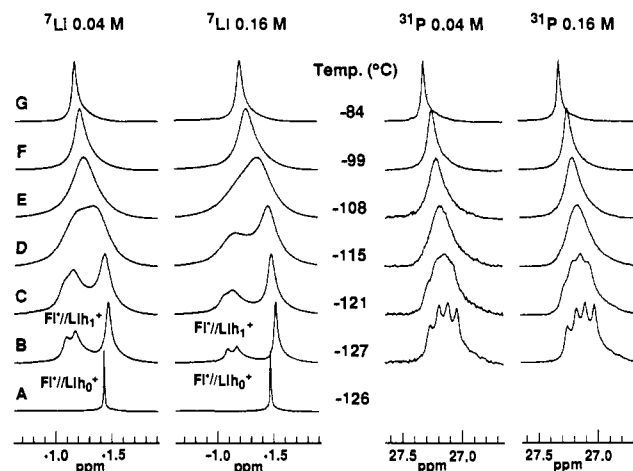


**Figure 2.** Variable temperature NMR spectra of 0.04 and 0.16 M 1Li at 0.5 equiv of HMPA.

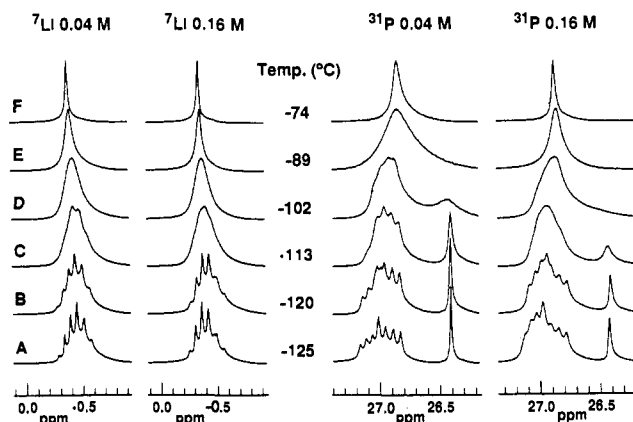


**Figure 3.** Variable temperature NMR spectra of 0.04 and 0.16 M 1Li at 4.0 equiv of HMPA.

A recent paper on the solid-state NMR (cross-polarization/magic angle spinning (CP/MAS)) of lithium fluorenyl<sup>16b</sup> reveals that  $\text{Li}^+$  is symmetrically disposed over the five-membered ring, the area of maximum shielding, for the THF complex. Cox et al. have made estimates of the distance between fluorenyl and lithium cation for different solvents.<sup>17</sup> The plot of  $^7\text{Li}$  chemical shift vs the estimated distance ( $\text{\AA}$ ) between the two ions gives a linear relationship.

The  $^{31}\text{P}$  NMR spectra are less informative, but fully support the assignments made by analysis of the  $^7\text{Li}$  spectra. Since lithium-7 has a spin of  $3/2$ , the lithium-coupled phosphorus signals are 1:1:1:1 quartets. All separated ions show the same trends in  $^{31}\text{P}$  chemical shifts and couplings as does lithium fluorenyl: the mono, bis, and tris HMPA complexes move progressively upfield, and the tetra moves downfield. The  $^2J_{\text{P-Li}}$  values decrease gradually as one to three HMPA molecules are coordinated to lithium (11.1–9.3 Hz); the coupling for  $1^-/\text{LiH}_4^+$  is noticeably smaller (7.7 Hz).

**Variable Temperature and Concentration Studies of Fluorenyllithium.** Variable temperature experiments on 0.04 and 0.16 M fluorenyllithium were carried out in the hope of gaining insight into the mechanism of exchange between  $1^-/\text{LiH}_0^+$  and  $1^-/\text{LiH}_1^+$  (0.5 equiv of HMPA, Figure 2) and between  $1^-/\text{LiH}_3^+$  and  $1^-/\text{LiH}_4^+$  (4.0 equiv of HMPA, Figure 3). (The temperature reported in the figures is an average of the temperature of the probe before the 0.04 M  $^7\text{Li}$  spectrum was taken and after the 0.16 M  $^{31}\text{P}$  spectrum was taken, typically a range of  $<1\text{ }^{\circ}$ .) The

(16) (a) Sethson, I.; Eliasson, B.; Edlund, U. *Magn. Reson. Chem.* **1991**, *29*, 1012. (b) Johnels, D.; Edlund, U. *J. Am. Chem. Soc.* **1990**, *112*, 1647.

(17) Cox, R. H.; Terry, H. W., Jr.; Harrison, L. W. *J. Am. Chem. Soc.* **1971**, *93*, 3297.

(15) Hoffmann, D.; Bauer, W.; Schleyer, P. v. R. *J. Chem. Soc., Chem. Commun.* **1990**, 208.

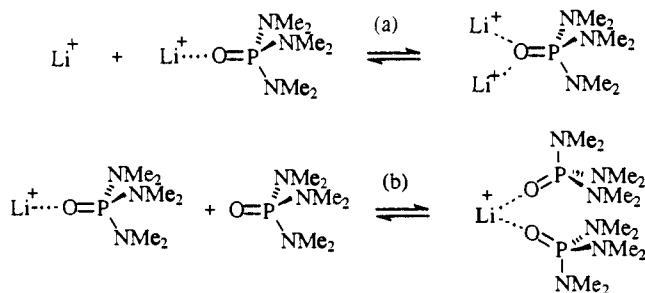


Figure 4. Possible bimolecular mechanisms for HMPA exchange.

spectra define the temperature range in which the Li–P couplings, which are the subject of this paper, can be observed (see also Figure 11).

The experiments in Figure 2 (0.5 equiv of HMPA) were an attempt to determine if the slow step for exchange of HMPA was unimolecular dissociation of coordinated HMPA in  $\text{LiH}_1^+$  or bimolecular association of two lithium cations ( $\text{LiH}_0^+ + \text{LiH}_1^+$ ), involving an HMPA bridging two lithiums (Figure 4, reaction a). This type of coordination has been observed in a  $(\text{LiBr})_2 \cdot (\text{HMPA})_3$  structure in the nonpolar medium toluene,<sup>5a</sup> but not in THF solution. The spectra were not subjected to quantitative line shape DNMR analysis to determine rate constants, but they provide strong qualitative evidence that the exchange rate of  $\text{LiH}_0^+$  with  $\text{LiH}_1^+$  at two concentrations differing by a factor of 4 is essentially the same (if anything, the low concentration spectra show more line broadening). Thus, the exchange proceeds by unimolecular dissociation of HMPA or bimolecular displacement of HMPA by solvent and not by direct transfer of HMPA between lithium cations.

The experiments at 4 equiv of HMPA (Figure 3), where  $\text{LiH}_3^+$  and  $\text{LiH}_4^+$  are the principal species, are less clear-cut. The 0.16 M spectra are consistently broader, and the coalescence with HMPA occurs at a lower temperature. A bimolecular mechanism for the exchange between  $\text{LiH}_3^+$  and  $\text{LiH}_4^+$ , such as depicted in Figure 4, reaction b, predicts that the lifetime of HMPA and  $\text{LiH}_3^+$  would be concentration dependent (as observed), whereas that of  $\text{LiH}_4^+$  should not be (the spectra do show some concentration dependence for  $\text{LiH}_4^+$ ). However, the solutions at 0.16 M are noticeably more viscous than those at 0.04 M, and some of the effects seen could result from this factor. We conclude cautiously that a bimolecular mechanism for exchange involving free HMPA is operative when excess HMPA is present.

These spectra also allow us to contrast the quite different effects of  $T_1$  and  $T_2$  broadening on the appearance of  $^{31}\text{P}$  signals coupled to  $^7\text{Li}$ . An important analysis of  $T_1$ -broadened signals has been reported by Bacon, Gillespie, and Quail.<sup>18</sup> Exchange ( $T_2$ ) broadened spectra show a more or less simultaneous coalescence of all four lines of the 1:1:1:1 quartet, as seen in Figures 2 and 3, whereas quadrupolar ( $T_1$ ) broadening shows first a characteristic coalescence of the pairs of outer lines to form a broad doublet (as seen for  $\text{Ph-LiH}_1$  (Figure 19)). Sometimes the sharp triplet of natural abundance  $^6\text{Li}$  can be seen in the valley of the doublet, as in the spectra of several lithium carbenoids published by Seebach<sup>11a</sup> and (tri-*tert*-butylphenyl)lithium by Schleyer.<sup>2a</sup>

**Effect of Diisopropylamine.** One of the great benefits of the technique being described in this paper for studying ion pair properties is the relative simplicity and convenience of the procedure. We have frequently prepared solutions of lithium reagents by metalation or other reaction with one of the butyllithiums, phenyllithium, or methylolithium, with the choice made on the basis of metalating ability and interference of the solvents and byproducts in the NMR spectra (particularly  $^{13}\text{C}$  interferences can be troublesome). However, in several cases the use of lithium diisopropylamide is advantageous, and this raises

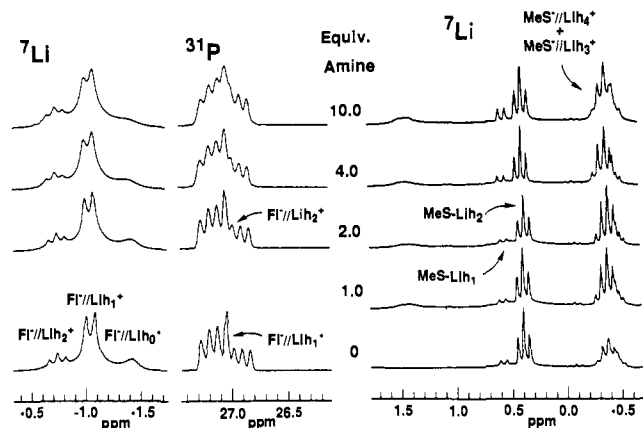


Figure 5.  $^7\text{Li}$  and  $^{31}\text{P}$  NMR spectra of  $1\text{Li}$  (0.16 M,  $-125^\circ\text{C}$ ) at 1.0 equiv of HMPA and  $\text{MeSLi}$  (0.16 M,  $-130^\circ\text{C}$ ) at 3.0 equiv of HMPA, with increasing quantities of diisopropylamine.

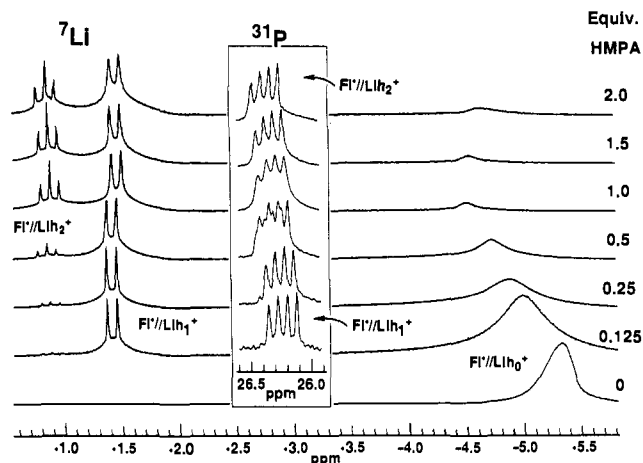


Figure 6. HMPA titration of 0.16 M fluorenyllithium ( $1\text{Li}$ ) in 20:1 ether/hexane at  $-121^\circ\text{C}$ .

the question of whether either the lone pair or hydrogen bond donor properties of diisopropylamine, which is formed during the metalation, interferes with the technique. Figure 5 shows the effect of added diisopropylamine to lithium fluorenyl at 1 equiv of HMPA and to  $\text{MeSLi}$  at 3 equiv. There appear to be only line width effects with the separated  $\text{LiH}_0^+$ ,  $\text{LiH}_1^+$ , or  $\text{LiH}_2^+$  of the lithium fluorenyl spectra. More substantial effects are seen for  $\text{MeSLi}$ : separated ions increase at the cost of monomer ions (see Figures 14 and 15 for a complete analysis of  $\text{MeSLi}$ ). It seems, therefore, that lithium reagents produced with LDA can be studied, but that the diisopropylamine may interfere with quantitative analysis.

**Fluorenyllithium in Ether.** We now contrast fluorenyllithium in THF with the very different behavior seen in ether. Fluorenyllithium is a contact species in ether ( $8^\circ\text{C}$ , 0.6 M),<sup>14d,15,16</sup> but at the low temperatures that are needed for our experiment it is poorly soluble.<sup>19</sup> The  $^7\text{Li}$  chemical shift at room temperature has been reported as  $\delta -6.2$ <sup>20</sup> and  $\delta -6.95$ <sup>17</sup> (reference: external aqueous  $\text{LiCl}$ ). The cause of the large upfield shift has been proposed to be shielding by the  $\pi$ -system.

Figure 6 shows the  $^7\text{Li}$  and  $^{31}\text{P}$  spectra of fluorenyllithium in ether at about  $-121^\circ\text{C}$ . First note the remarkable upfield shift of the  $^7\text{Li}$  signal in the contact ion pair at 0 equiv of HMPA: the chemical shift is  $\delta -5.4$  relative to an external 0.3 M  $\text{LiCl}$  ( $\text{MeOH}$ )

(19) It is interesting to note that 0.6 M fluorenyllithium in ether precipitates at  $0^\circ\text{C}$ .<sup>15</sup> We were able to observe the contact species by low-temperature  $^7\text{Li}$  NMR before crystallization occurred. The addition of HMPA greatly retarded the formation of crystals.

(20) Dixon, J. A.; Gwinner, P. A.; Lini, D. C. *J. Am. Chem. Soc.* **1965**, *87*, 1379.

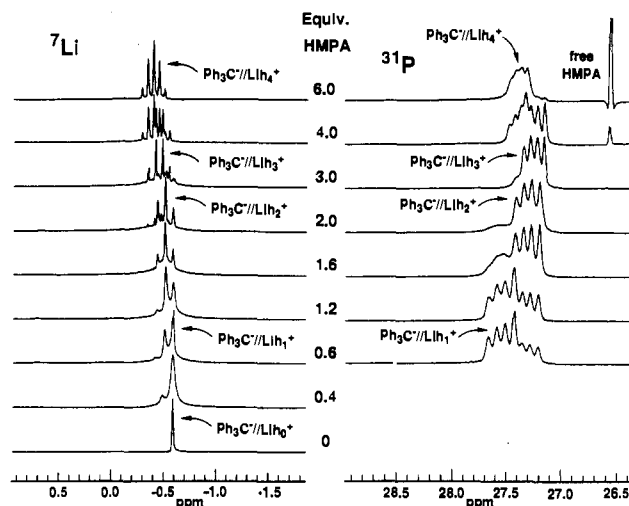


Figure 7. HMPA titration of 0.16 M trityllithium (**2Li**) in 3:2 THF/ether at  $-129$  °C.

reference at  $-121$  °C. The difference in chemical shift between the earlier values and this value is probably due to different reference standards and the low temperature of our experiment, which may have produced a higher concentration of SSIP.

As HMPA was added, two new lithium signals, a doublet ( $1^-//\text{LiH}_1^+$ ) and triplet ( $1^-//\text{LiH}_2^+$ ), were observed at  $\delta -1.44$  and  $-0.90$ , respectively. These signals were sharp and close in chemical shift to similar ions in THF. Interestingly, the contact  $^7\text{Li}$  signal gradually moved downfield as HMPA was added, possibly due to a dynamic equilibrium between **1Li** and an unobservable species such as an ether-solvated separated ion. Such an equilibrium ( $T_2$  broadening) may also explain the very broad contact peak observed, although a substantial inherent line width for a contact species could simply be due to  $T_1$  relaxation. The  $^{31}\text{P}$  NMR spectra reveal that, unlike the HMPA titration of fluorenyllithium and all other separated ions we have observed in THF, the  $^{31}\text{P}$  signal for  $1^-//\text{LiH}_1^+$  is *upfield* of  $1^-//\text{LiH}_2^+$ , which suggests that the magnetic anisotropy effects of fluorenyl are more important in ether than in THF.

Finally, the addition of 1–2 equiv of HMPA caused an increasing amount of precipitate, until at 3 equiv of HMPA no NMR signal could be detected. This precipitate was insoluble even at room temperature and only completely dissolved with greater than 16 equiv of HMPA. The source of the precipitate is probably  $1^-//\text{LiH}_3^+$  which must be insoluble in ether, since no  $1^-//\text{LiH}_3^+$  quartet was detected. The low solubility of  $R^-//\text{LiH}_3^+$  in ether is not a general phenomenon.

**Trityllithium.** Trityllithium (**2Li**) has been studied by UV spectroscopy,<sup>21</sup>  $^1\text{H}$  NMR,<sup>14d,22</sup>  $^{13}\text{C}$  NMR,<sup>14c,23</sup>  $^7\text{Li}$  NMR,<sup>23</sup> and X-ray crystallography.<sup>24</sup> The  $^1\text{H}$  NMR work of Jackman et al.<sup>14d</sup> and the  $^{13}\text{C}$  NMR work of O'Brien et al.<sup>14c</sup> demonstrate that trityllithium is solvent-separated even at  $50$  °C in THF. Low temperatures generally favor separated ions.<sup>4a,14a</sup>

Examination of  $^7\text{Li}$  and  $^{31}\text{P}$  NMR spectra for the addition of HMPA to trityllithium in Figure 7 demonstrates the similarities between fluorenyllithium and trityllithium. In the  $^7\text{Li}$  NMR spectra, the progression from a singlet ( $\nu_{1/2} = 3$  Hz) at 0 equiv of HMPA to a  $^{31}\text{P}$ -coupled  $^7\text{Li}$  quintet closely follows the sequence found for fluorenyllithium. One observed difference is the narrow chemical shift range of the lithium signals for  $\text{LiH}_0^+$ ,  $\text{LiH}_1^+$ ,  $\text{LiH}_2^+$ ,  $\text{LiH}_3^+$ , and  $\text{LiH}_4^+$  (0.24 ppm) as compared to fluorenyllithium (0.93 ppm). Thus, the "propeller" shape of the three aryl rings<sup>24</sup> does not cause the strong magnetic anisotropy effects seen for

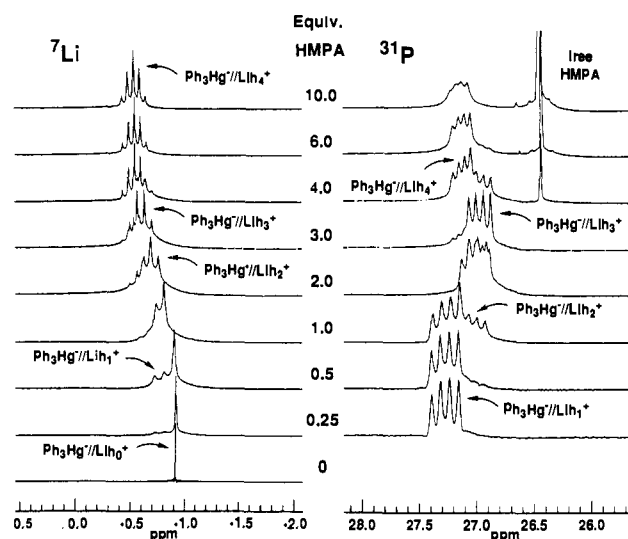
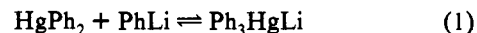


Figure 8. HMPA titration of 0.16 M  $\text{Ph}_3\text{HgLi}$  (**3Li**) in THF at  $-120$  °C.

fluorenyl. The chemical shifts of  $\text{LiH}_3^+$  and  $\text{LiH}_4^+$  are very similar to those of fluorenyllithium. Therefore, even in fluorenyllithium, the lithiums of  $\text{LiH}_3^+$  and  $\text{LiH}_4^+$  are outside the magnetic anisotropy of the aromatic fluorenyl.

The  $^{31}\text{P}$  NMR of the HMPA titration of trityllithium reveals that the relative chemical shifts of  $\text{LiH}_1^+$ ,  $\text{LiH}_2^+$ ,  $\text{LiH}_3^+$ , and  $\text{LiH}_4^+$  in THF are the same as for fluorenyllithium ( $\delta \text{LiH}_1^+ > \text{LiH}_2^+ > \text{LiH}_4^+ > \text{LiH}_3^+$ ) and that the complete conversion of  $\text{LiH}_3^+$  to  $\text{LiH}_4^+$  requires an excess ( $\sim 6$  equiv) of HMPA.

**Mercury "Ate" Complex.** The last example of a solvent-separated ion pair is the triphenylmercury "ate" complex, **3Li**, formed by addition of  $\text{PhLi}$  to diphenylmercury in THF (eq 1). Our interest in this species, as well as related ate complexes of iodine,<sup>1a,c,g</sup> tellurium,<sup>1c,g</sup> selenium,<sup>1h</sup> and tin<sup>1i</sup> originated in its possible role as an intermediate in the  $\text{Li}/\text{Hg}$  transmetalation reaction. Several kinds of organomercury ate complexes have been proposed as intermediates.<sup>25</sup> Silyl and germyl mercury ate complexes have been characterized in solution and by X-ray crystallography.<sup>26</sup> Attempts to detect  $\text{Ph}_3\text{HgLi}$  in ether by colligative techniques were unsuccessful.<sup>27</sup> We have recently reported that  $\text{Ph}_3\text{HgLi}$  forms in THF and have used it as a spectroscopic model for  $\text{Ph}_2\text{ILi}$  and  $\text{Ph}_3\text{TeLi}$ .<sup>18</sup>



In Figure 8, the  $^7\text{Li}$  and  $^{31}\text{P}$  spectra for the HMPA titration of **3Li** are presented. The chemical shift range of the various species in the  $^7\text{Li}$  spectra is similar in magnitude to that of fluorenyllithium; therefore, all of the different lithium species are clearly identifiable. We speculate that the somewhat greater shift dispersion for **3Li** compared to **2Li** results from the greater planarity of the phenyl groups in the former. Trityl is known to have a propeller shape, and perhaps the long C–Hg bonds allow coplanarity. As in fluorenyl- and trityllithium, the  $^7\text{Li}$  chemical shifts of  $\text{LiH}_0^+$ ,  $\text{LiH}_1^+$ , and  $\text{LiH}_2^+$  are sensitive to the counter ion, whereas the chemical shifts of  $\text{LiH}_3^+$  and  $\text{LiH}_4^+$  are practically unaffected. Except for small shift differences of  $\text{LiH}_1^+$  and  $\text{LiH}_2^+$ , the  $^{31}\text{P}$  spectra are virtually identical to the  $^{31}\text{P}$  spectra of the other solvent-separated systems.

**Other Ate Complexes.** We have previously reported the HMPA titration of a boron ate complex,  $\text{Et}_3\text{PhBLi}$ .<sup>1b</sup> In addition, the ate complexes  $\text{Ph}_3\text{TeLi}$ ,<sup>1c</sup>  $\text{Ph}_2\text{ILi}$  (**4Li**),<sup>1a,c</sup> and others show nearly

(21) Buncel, E.; Menon, B. *J. Org. Chem.* **1979**, *44*, 317.

(22) Sandel, V. R.; Freedman, H. H. *J. Am. Chem. Soc.* **1963**, *85*, 2328.

(23) Waack, R.; Doran, M. A.; Baker, E. B.; Olah, G. A. *J. Am. Chem. Soc.* **1966**, *88*, 1272.

(24) Brooks, J. J.; Stucky, G. D. *J. Am. Chem. Soc.* **1972**, *94*, 7333.

(25) Seitz, L. M.; Hall, S. D. *J. Organomet. Chem.* **1968**, *15*, C7.

(26) Schaaf, T. P.; Oliver, J. P. *J. Am. Chem. Soc.* **1969**, *91*, 4327.

(27) Wittig, V. G.; Meyer, F. J.; Lange, G. *Justus Liebigs Ann. Chem.* **1951**, *571*, 167.

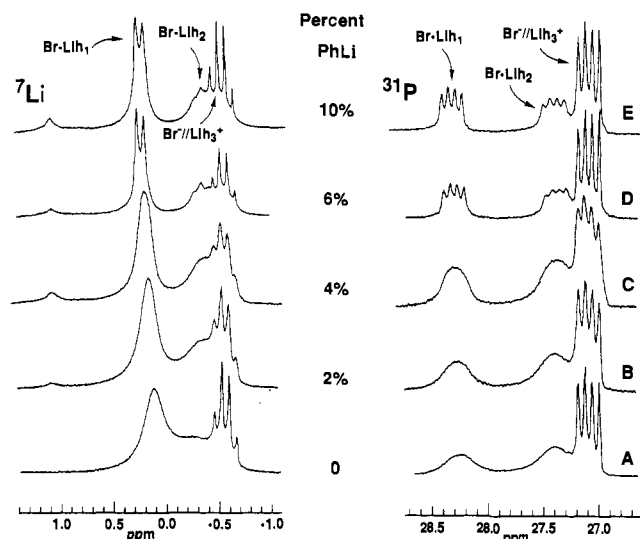


Figure 9. PhLi titration of 0.08 M lithium bromide in THF below  $-110^{\circ}\text{C}$  with 2.0 equiv of HMPA.

identical HMPA titration behavior. We will not present that information here.

**Summary of Separated Ion Spectral Characteristics.** The above analysis has demonstrated that each  $\text{LiH}_n^+$  cation can be separately identified in both the  $^7\text{Li}$  and  $^{31}\text{P}$  NMR spectra. Key points in the titration are the following: (1) the formation of a 20:60:20 mixture of  $\text{LiH}_n^+$ ,  $n = 0, 1, 2$ , when 1 equiv of HMPA has been added; (2) the formation of almost pure  $\text{LiH}_3^+$  when 3 equiv of HMPA has been added; (3) the formation of  $\sim 1:1$   $\text{LiH}_3^+$  and  $\text{LiH}_4^+$  at 4 equiv of HMPA (i.e., the last equivalent of HMPA is bound weakly); (4) the quite characteristic *relative* chemical shifts of  $^7\text{Li}$ , and particularly of the  $^{31}\text{P}$  signals. Although only three separated ions have been presented above, we have found very consistent chemical shift behavior for separated ions formed from several dozen carbanions and other anions during HMPA titrations.

We will use these points as a "signature" for a separated ion pair.

### Separable Contact Ion Pairs

In the discussion above we have shown that several separated lithium ion pairs behave in a characteristic and easily recognized fashion when increments of HMPA are added. We now discuss systems which are all or mostly contact in THF and which separate when HMPA is added. A set of criteria will be established for recognizing both contact ions and the contact to separated transition. We will deal with lithium methaneselenolate and methanethiolate and the lithium halides (except for lithium fluoride, which is insoluble even with a large excess of HMPA). These illustrate some periodic trends and span the range of lithium salts from weakly contact to aggregated in THF.

**Exchange Broadening in the Lithium Halides.** Oven- and/or vacuum-dried samples of LiCl, LiBr, and LiI gave broad, unrecognizable NMR signals for all contact species during a typical HMPA titration (separated ions formed were considerably sharper and showed Li-P coupling). This complicated our study of the behavior of these salts in THF/HMPA mixtures (Figure 9A, 2 equiv of HMPA). An explanation for the broadening and a procedure for obtaining sharp spectra were developed when we observed that well-resolved peaks for  $\text{Br-LiH}_n$  ( $n = 1$  and  $2$ ) were observable in 1:1 LiBr/PhLi.<sup>1b</sup> We hypothesized that broadening is the result of a *catalyzed* exchange of coordinated HMPA, where the catalyst is some protic impurity in the LiBr, possibly water. In fact, when small increments of PhLi were added to a LiBr/THF/HMPA solution (Figure 9), the peaks sharpened. As a result, we studied LiI, LiBr, and LiCl in THF solutions

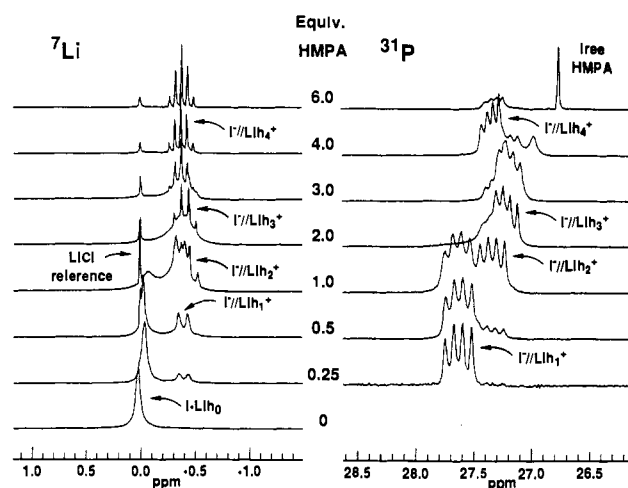


Figure 10. HMPA titration of lithium iodide in 3:2 THF/ether at  $-123^{\circ}\text{C}$  with 0.3 M LiCl/MeOH external reference (capillary insert).

containing a small amount ( $\approx 10\%$ ) of PhLi or LDA, which appears to effectively suppress the intermolecular exchange of various ion pair species. Dry solutions of LiI, LiBr, and LiCl were also generated through the reaction of methylolithium with iodomethane, 1,2-dibromoethane, or trimethylchlorosilane.

**Lithium Iodide.** Lithium iodide is monomeric in THF at room temperature.<sup>28</sup> The HMPA titration (Figure 10) is somewhat more ambiguous than the other systems discussed here. In THF, a broad signal at 0.01 ppm is observed downfield of the usual separated ion position of  $-0.5$  to  $-1.5$  ppm and suggests a contact species, I-LiH<sub>0</sub>. Fully separated ions in THF usually give sharp  $^7\text{Li}$  signals, showing neither  $T_1$  nor  $T_2$  broadening. The I-LiH<sub>0</sub> signal underwent a small upfield shift as its concentration decreased during the titration, as can be seen in Figure 10, which shows spectra taken with an external LiCl/MeOH reference capillary in the NMR tube. The chemical shift of LiI in THF is also temperature dependent, which may indicate the coexistence of significant amounts of contact and separated ion pairs in dynamic equilibrium, or perhaps monomers and dimers. If the former is true, then the easy ion separation on addition of HMPA is not very surprising. The HMPA complex closely resembles those of known separated ions except for the slightly anomalous Li and P signals of I//LiH<sub>1</sub><sup>+</sup> (the  $^7\text{Li}$  doublet of R//LiH<sub>1</sub><sup>+</sup> is usually slightly upfield of the triplet of R//LiH<sub>2</sub><sup>+</sup>). We think it most likely that coordination of the first equivalent of HMPA causes partial ion separation of the weakly coordinated iodide. Incomplete ion separation of I-LiH<sub>1</sub> is also indicated by a higher than normal temperature dependence of the  $^7\text{Li}$  shift. If the mono HMPA complex is a mixture of CIP and SIP, then equilibration between them ( $\text{I-LiH}_1 \rightleftharpoons \text{I//LiH}_1^+$ ) must be fast on the NMR time scale at  $-140^{\circ}\text{C}$ , since only a single doublet was observed.

**Temperature Effects.** Line widths in  $^7\text{Li}$  and  $^{31}\text{P}$  NMR spectra vary with temperature in a complex fashion, with both nuclei not optimal at any single temperature. Figure 11 illustrates this effect for LiI and MeSeLi. In general,  $^{31}\text{P}$  signals in 3:2 THF/ether show less well-resolved splitting at low temperatures ( $< -130^{\circ}\text{C}$ ), whereas the  $^7\text{Li}$  signals improve steadily until the solvent freezes. The origin of this effect is not known, but is probably related to the viscosity of the medium, since similar problems were not encountered when dimethyl ether was substituted for ether. Figure 18 illustrates this change for lithium chloride.

**Lithium Bromide.** Lithium bromide (0.03 M) at  $37^{\circ}\text{C}$  is about 80% monomeric and 20% higher aggregates in THF ( $\text{MW}_{\text{app}}/\text{MW}_{\text{real}} = 1.23$ ).<sup>28</sup> Our interpretation of the HMPA titration of LiBr (0.2 M) in 3:2 THF/ether (Figure 12) is as follows. The  $^7\text{Li}$  chemical shift ( $\delta 0.65$ ) indicates that Br-LiH<sub>0</sub> is a contact ion.

(28) Wong, M. K.; Popov, A. I. *J. Inorg. Nucl. Chem.* 1972, 34, 3615.

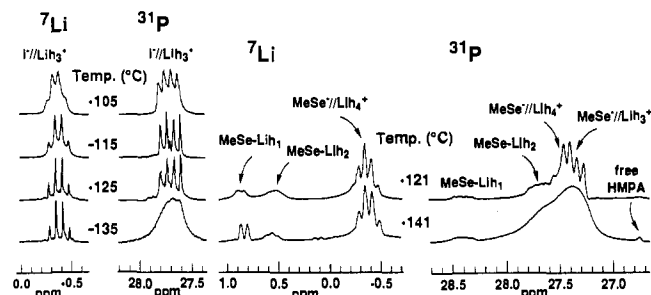


**Figure 11.** Temperature dependence of lithium iodide (left) and MeSeLi (right) in 3:2 THF/ether with 3.0 equiv of HMPA.

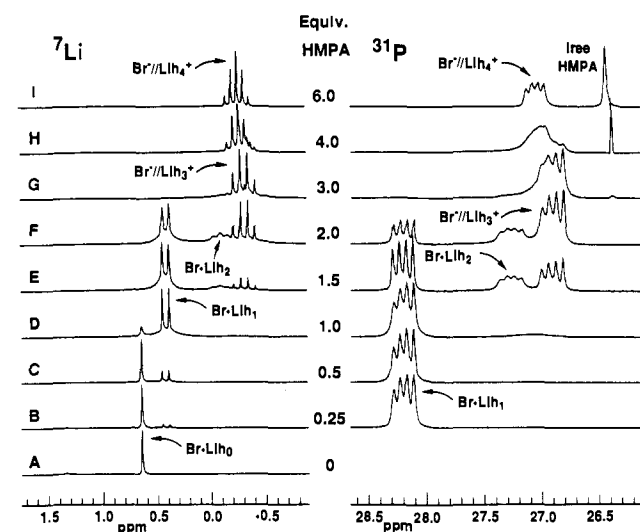


**Figure 12.** HMPA titration of 0.20 M lithium bromide in 3:2 THF/ether at  $-130\text{ }^{\circ}\text{C}$ .

The first equivalent of HMPA produces a single new species ( $\delta_{\text{Li}}$  0.42,  $\delta_{\text{P}}$  28.19, 1:1:1:1 q) which is a mono HMPA complex,  $\text{Br-//Lih}_1$ . Since LiBr in THF is probably mostly monomeric (it is at room temperature<sup>28</sup> but has not been studied at  $-123\text{ }^{\circ}\text{C}$ ), the  $\text{Br-//Lih}_1$  species is monomeric. The chemical shifts of  $\text{Br-//Lih}_1$  are sufficiently different from those observed for any of the separated ions that we can confidently assign a contact ion pair structure to it. Further evidence is provided by the observation that at 2.0 equiv of HMPA the mono- and tricoordinated complexes ( $\text{Br-//Lih}_1$  and  $\text{Br-//Lih}_3^+$ ) coexist in almost equimolar amounts (see Figure 12F), which was not seen for any of the separated ions (these are predominantly  $\text{R-//Lih}_2^+$  at this stage). In other words,  $\text{Br-//Lih}_1$  is substantially less electrophilic than the separated ion  $\text{Lih}_1^+$ , thus allowing the formation of some  $\text{Lih}_3^+$  while  $\text{Br-//Lih}_1$  is still present. This is exactly what would be expected for the contact ion, since  $\text{Br}^-$  is clearly a better donor ligand than THF.

The second contact species formed ( $\text{Br-//Lih}_2$ ,  $\delta_{\text{Li}}$   $-0.08$ ,  $\delta_{\text{P}}$  27.31) cannot be identified as easily as  $\text{Br-//Lih}_1$  since the chemical shifts of  $\text{Br-//Lih}_2$  are similar to those of solvent-separated ions. Nevertheless, we feel confident that it is a contact ion. The Li shift of  $\text{Br-//Lih}_2$  is *downfield* of  $\text{Br-//Lih}_3^+$ , whereas for all separated ions,  $\text{R-//Lih}_2^+$  is *upfield* of  $\text{R-//Lih}_3^+$ . In addition, the  $^{31}\text{P}$  signal of  $\text{R-//Lih}_2^+$  is *downfield* of  $\text{R-//Lih}_3^+$  by  $<0.1$  ppm, whereas the  $\text{Br-//Lih}_2$  signal is *downfield* of the  $\text{Br-//Lih}_3^+$  signal by 0.4 ppm. Furthermore, careful inspection of Figure 12G reveals that (1)  $\text{Br-//Lih}_2$  is still present when excess HMPA appears and (2) at slightly higher temperature (not shown) it is dynamically broadened by exchange with free HMPA. Neither is true for separated  $\text{R-//Lih}_2^+$ .

The third species formed from lithium bromide is  $\text{Br-//Lih}_3^+$ , on the basis that the coupling constant, chemical shift, and line width are all virtually identical to those observed for other

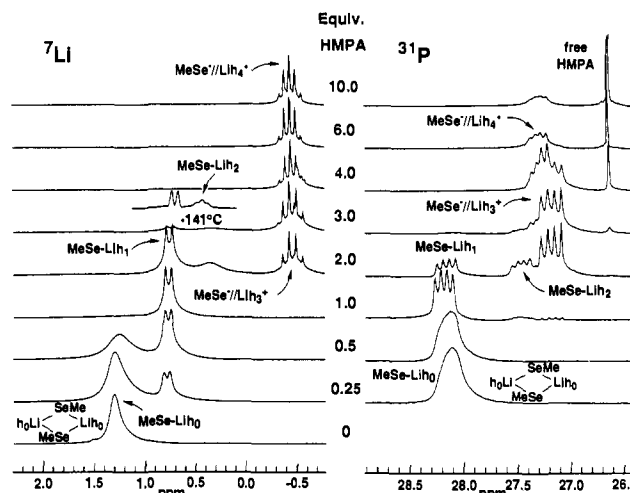


**Figure 13.** HMPA titration of 0.16 M MeSeLi in 20:1 THF/hexane at  $-124\text{ }^{\circ}\text{C}$ . Spectra are plotted at the same frequency scale. Inset at 3 equiv of HMPA in 3:2 THF/ether at  $-141\text{ }^{\circ}\text{C}$ .

$\text{R-//Lih}_3^+$  species (e.g., **1Li**, **2Li**, **3Li**, and lithium iodide). Thus, coordination of the third HMPA ligand causes ejection of the bromide ion. Further increments of HMPA produce effects that are very similar to those observed for all other separated  $\text{Lih}_3^+$  and  $\text{Lih}_4^+$  ions (e.g., at 4 equiv of HMPA only 3.5 equiv of HMPA is complexed and 0.5 equiv is free). The coexistence of  $\text{R-//Lih}_n$  and  $\text{R-//Lih}_{n+2}^+$  species as shown for LiBr ( $n = 1$ ) has turned out to be a useful characteristic for identifying the transition from contact to separated ion pairs and has been seen for a number of other lithium compounds.

**Lithium Methaneselenolate.** The similarity between the  $^7\text{Li}$  and  $^{31}\text{P}$  NMR spectra of MeSeLi (Figure 13) and LiBr (Figure 12) is striking: both possess a double HMPA coordinated contact species ( $\text{Br-//Lih}_2$  or  $\text{MeSe-//Lih}_2$ , see 2.0 equiv), both ionize to roughly the same extent with the addition of HMPA, and both have very similar Li and P chemical shifts. This parallel behavior is not too surprising since selenium and bromine are in the same period. There is one important difference: the  $\text{MeSe-//Lih}_0$  lithium signal is quite broad. Lithium NMR signals can be broadened by dynamic exchange ( $T_2$ ) and/or quadrupolar relaxation ( $T_1$ ) processes. The broadening of  $\text{MeSe-//Lih}_0$  is indicative of the  $T_2$  type, which shows a strong temperature and concentration dependence and may be caused by dynamic exchange with some dimer ( $2\text{MeSeLi} \rightleftharpoons (\text{MeSeLi})_2$ ). The broadening observed in the  $^7\text{Li}$  spectrum of the  $\text{MeSe-//Lih}_2$  signal at 2 equiv ( $\delta$  0.3) also appears to be mainly of the  $T_2$  type, since at very low temperatures ( $-141\text{ }^{\circ}\text{C}$ , inset in Figure 13) the signal sharpens to a triplet.

**Lithium Methanethiolate.** Although no aggregation studies have been reported in THF for MeSLi, it would be expected to be more aggregated than MeSeLi and probably lithium chloride (higher charge density and/or more basic). Since lithium chloride is principally a dimer at  $37\text{ }^{\circ}\text{C}$  in THF,<sup>28</sup> MeSLi should also be aggregated. An HMPA titration of aggregates can potentially lead to a more complex array of ions than observed in the lithium salts discussed so far. Indeed, rather complex behavior has been reported for HMPA titrations of aggregated lithium amides<sup>6</sup> and phenoxides<sup>7</sup> in THF.

In order to properly characterize the various ion pairs of MeSLi formed during the titration, both  $^7\text{Li}$  and  $^6\text{Li}$  NMR spectra were observed, studies were performed in both THF and THF/ether at the very lowest accessible temperatures, and variable concentration studies were carried out. The effects of using  $^6\text{Li}$  instead of  $^7\text{Li}$  are compared in Figures 14 and 15. Especially advantageous is the better separation of  $^{31}\text{P}$  chemical shifts (see Figure 15) due to the fact that the  $^6\text{Li}$ -coupled phosphorus signals are narrower than  $^7\text{Li}$ -coupled signals by a factor of 4. The usual line-narrowing effect of  $^6\text{Li}$  over  $^7\text{Li}$  is not clearly evident here, consistent with



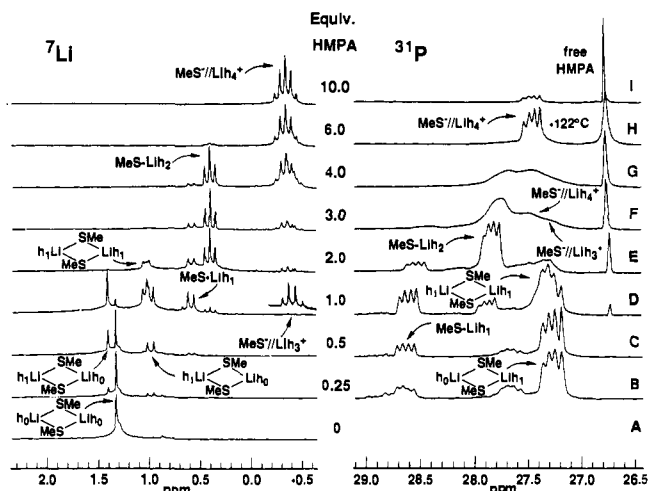


Figure 14. HMPA titration of 0.16 M MeSLi in 3:2 THF/ether at  $-138$  °C.

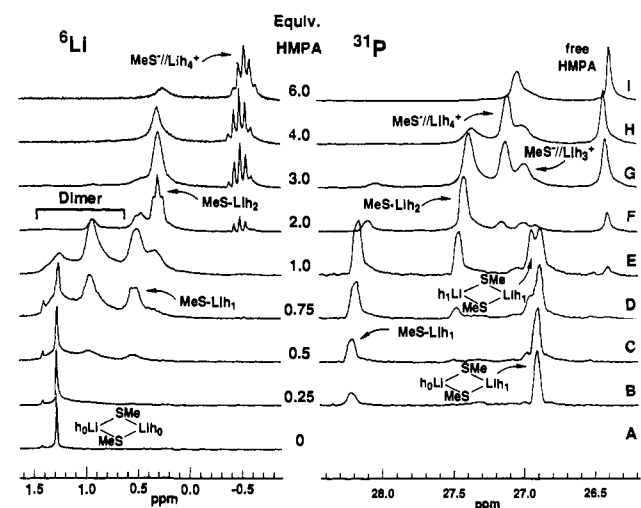


Figure 15. HMPA titration of 0.16 M MeS<sup>6</sup>Li in 20:1 THF/hexane at  $-124$  °C. Plotted frequency scale ratio  ${}^6\text{Li}:$  ${}^{31}\text{P}$  is 1:2.

our conclusion that dynamic exchange ( $T_2$ ) among ion pairs is the main broadening process. This has the consequence that the smaller  ${}^{31}\text{P}$ - ${}^6\text{Li}$  couplings are actually harder to resolve than those of  ${}^7\text{Li}$ .

The HMPA titration of MeSLi is complex. At 0.25 equiv of HMPA (Figure 14B), two prominent  ${}^{31}\text{P}$  signals are observed: the upfield signal ( $\delta$  27.28) is assigned to a dimeric species,  $(\text{MeSLi})_2\text{h}_1$  (see Figure 16), and the downfield signal ( $\delta$  28.62) to a monomeric species ( $\text{MeS-LiH}_1$ ). The impurity at  $\delta$  27.67 may be due to  $\approx 4\%$  lithium chloride present in the methyllithium used to prepare the thiolate. Support for the dimer/monomer assignment can be found in the  ${}^7\text{Li}$  NMR spectra from 0.25 to 1.0 equiv of HMPA. In the dimer region (1.6–0.9 ppm) a new singlet ( $\delta$  1.40) and doublet ( $\delta$  0.98) were observed, due to the same species. The latter peak is a dimer lithium with a coordinated HMPA, and the former a dimeric lithium with no coordinated HMPA;  $(\text{MeSLi})_2\text{h}_1$  is an obvious candidate. At 1 equiv of HMPA, a new doublet ( $\delta$  1.04) was observed due to a symmetric dimer species with one HMPA on each lithium ( $\text{MeSLi})_2\text{h}_2$  (see Figure 16). This assignment is supported by the appearance of a second dimer HMPA peak ( $\delta_{\text{P}}$  27.0) at 0.5, 0.75, and 1.0 equiv of HMPA in Figure 15C–E. These signals are poorly resolved in the  ${}^7\text{Li}$  spectra. The addition of more HMPA causes the dissociation of dimers and the formation of the monomeric species  $\text{MeS-LiH}_1$  ( $\delta_{\text{Li}}$  0.60, d) and  $\text{MeS-LiH}_2$  ( $\delta_{\text{Li}}$  0.40, t) in Figures 14

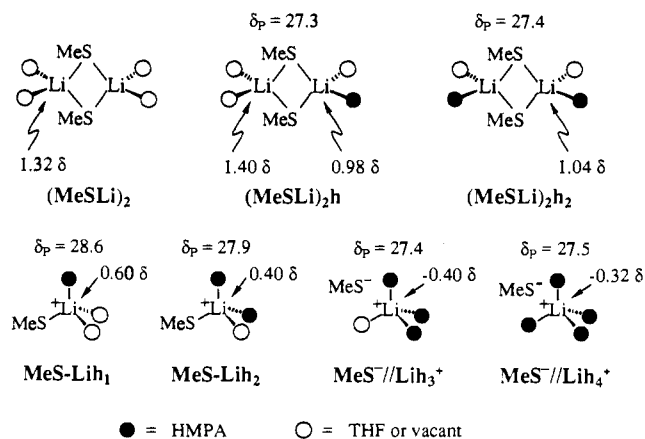


Figure 16.  ${}^7\text{Li}$  and  ${}^{31}\text{P}$  shifts of species formed during the HMPA titration of MeSLi in 3:2 THF/ether (Figure 14).

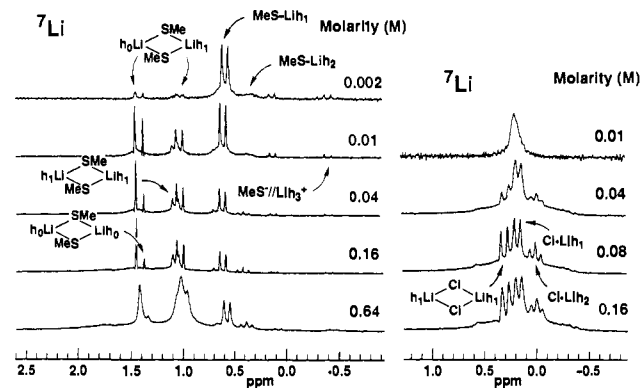


Figure 17. Concentration dependence of the  ${}^7\text{Li}$  NMR spectra of MeSLi ( $-138$  °C) and lithium chloride ( $-141$  °C) in 3:2 THF/ether at 1.0 equiv of HMPA.

and 15.<sup>29</sup> The corresponding  ${}^{31}\text{P}$  signals for  $\text{MeS-LiH}_1$  and  $\text{MeS-LiH}_2$  are clearly observed from 0.75 to 4.0 equiv of HMPA. The assignments of dimer and monomer signals were confirmed by a variable concentration experiment (Figure 17). At 0.64 M the principal species are dimers, at 0.002 M monomers.

The earliest indication of separated ion comes at 1.0 equiv of HMPA with the appearance of  $\text{MeS}^-//\text{LiH}_3^+$ . The small concentration of  $\text{MeS}^-//\text{LiH}_3^+$  makes it difficult to identify; however, the quartet can be seen at  $\delta$  -0.4 in the vertically expanded  ${}^7\text{Li}$  spectrum of Figure 14D, and the  ${}^{31}\text{P}$  signal can be seen at  $\delta$  27.0, just downfield of  $(\text{MeSLi})_2$  in Figure 15D. Between 2 and 6 equiv of HMPA, the separated ion is a mixture of  $\text{MeS}^-//\text{LiH}_3^+$  ( $\delta_{\text{Li}}$  -0.4, quartet) and  $\text{MeS}^-//\text{LiH}_4^+$  ( $\delta_{\text{Li}}$  -0.3, quintet), with  $\text{MeS}^-//\text{LiH}_4^+$  clearly visible as a well-resolved 1:1:1:1 quartet at  $-122$  °C in the  ${}^{31}\text{P}$  spectrum (Figure 14H). The qualitative ratio of  $\text{MeS}^-//\text{LiH}_3^+$  to  $\text{MeS}^-//\text{LiH}_4^+$  can best be seen in the  ${}^{31}\text{P}$  spectra of Figure 15F–H, which show that, in the presence of contact ion and free HMPA, the separated ion with the larger number of HMPA molecules will be favored.

Information about strength of the coordination between  $\text{MeS}^-$  and  $\text{Li}^+$  is provided by several features of this spectrum. In the titration of MeSLi, free HMPA is already observed at 1 equiv of HMPA, compared with 3 equiv or more for MeSeLi, LiI, or LiBr. The early appearance of free HMPA as well as  $\text{MeS}^-//\text{LiH}_4^+$  is characteristic of much stronger coordination between lithium and counterion for MeSLi.

**Lithium Chloride.** Vapor pressure osmometry gives  $MW_{\text{app}}/MW_{\text{real}}$  of 1.83 for lithium chloride in THF.<sup>28</sup> A crystal structure of  $(\text{LiCl})_4(\text{HMPA})_4$  has been reported.<sup>5c</sup> Even without this

(29) The chemical shifts in Figures 14 and 15 differ slightly because of the difference in solvent (external referencing was used): 3:2 THF/ether for Figure 14 and 95:5 THF/hexane for Figure 15.



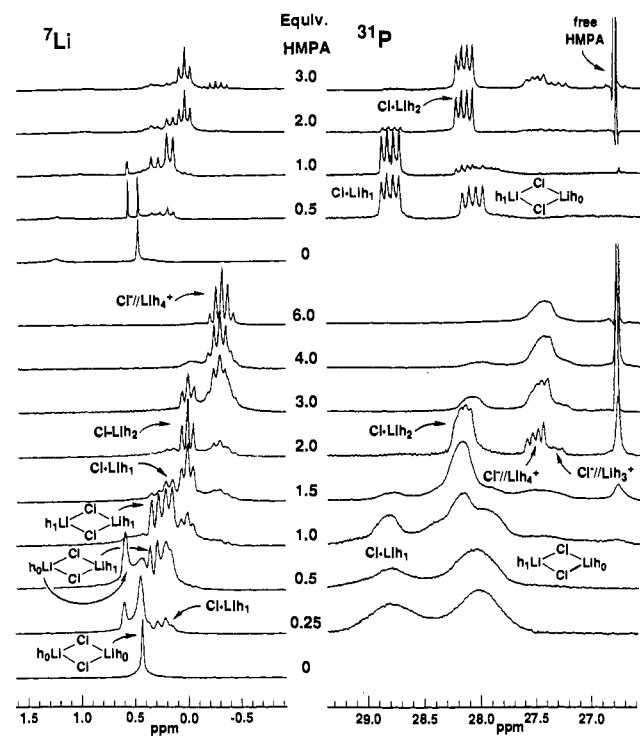


**Figure 18.** HMPA titration of lithium chloride: 0.16 M in 3:2 THF/ether at  $-142\text{ }^{\circ}\text{C}$  (lower titration) and 0.05 M in 1:1 THF/Me<sub>2</sub>O at  $-144\text{ }^{\circ}\text{C}$  (upper titration).

information, the HMPA titration of lithium chloride provides a multiplicity of species which can only be explained by aggregation. Structural assignments are provided in Figure 18. The progress of the titration is very similar to that reported above for MeSLi, and the detailed arguments will not be repeated here. The two closely spaced doublets in the 1 equiv of HMPA spectra were identified as (ClLi)<sub>2</sub>h<sub>1</sub> and Cl-LiH<sub>1</sub> on the basis of the increase in the upfield doublet at the expense of the downfield doublet and the Cl-LiH<sub>2</sub> triplet when the solution was diluted (Figure 17). In contrast, to the titration of MeSLi, distinct signals for (ClLi)<sub>2</sub>h<sub>1</sub> and (ClLi)<sub>2</sub>h<sub>2</sub> were not seen; their <sup>7</sup>Li doublets are probably superimposed.

We were unable to achieve well-resolved signals of lithium chloride in either THF or THF/ether solvent. The top portion of Figure 18 shows an HMPA titration in 1:1 THF/dimethyl ether, which gives very sharp signals in both <sup>7</sup>Li and <sup>31</sup>P NMR, even at temperatures as low as  $-144\text{ }^{\circ}\text{C}$ . Media containing a substantial fraction of dimethyl ether have been found to be superior to all others tried.<sup>2d,3,30b</sup> From qualitative observations, we place the polarity of dimethyl ether between that of pure THF and 3:2 THF/ether.

We categorize lithium chloride in THF as a sturdy dimer which complexes at least one HMPA without dissociating, but additional HMPA causes conversion to mono and bis HMPA complexed monomers and eventually, like the other systems reported above, to essentially fully separated ions.

### Inseparable Lithium Species

**Effect of HMPA on a Weakly Aggregated Localized Organolithium. Phenyllithium.** Phenyllithium is among the most intensively studied simple lithium reagents, with X-ray structures of a tetramer,<sup>31</sup> trimer (LiBr complex),<sup>31</sup> dimer,<sup>32</sup> and monomer.<sup>32</sup>

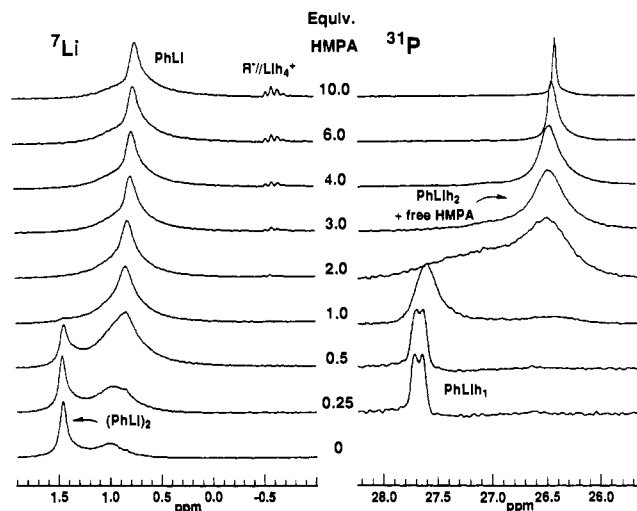


**Figure 19.** HMPA titration of 0.08 M PhLi in THF at  $-118\text{ }^{\circ}\text{C}$ .

There have also been extensive solution studies.<sup>1a,c,2a,11b,30,34</sup> In THF at 0.08 M concentration, PhLi is approximately a 1:1 mixture of dimer and monomer.<sup>1a,c,2a</sup> An HMPA titration of such a solution is presented in Figure 19.<sup>1a</sup> Addition of HMPA results in formation of only a monomeric contact Ph-LiH<sub>1</sub> species (no signals attributable to a dimeric HMPA complex were seen). There is indirect indication of Ph-LiH<sub>2</sub> formation, but it is in rapid exchange with free HMPA down to  $-118\text{ }^{\circ}\text{C}$ . Carbon-13 NMR spectra<sup>1a</sup> support these assignments. Only traces of separated ion are formed even in the presence of 10 equiv of HMPA. The small <sup>7</sup>Li quintet at  $\delta -0.55$  (Figure 19) may be from decomposition products since no corresponding <sup>13</sup>C NMR signals could be detected. The very early appearance of free HMPA is characteristic of lithium reagents with strong donor ligands.

**Effect of HMPA on a Strongly Aggregated Organolithium. Methyllithium.** We complete our survey of the effect of HMPA on lithium reagents with one whose behavior contrasts sharply with all of the systems discussed above. Methyllithium is tetramer in ether,<sup>35a</sup> the crystalline TMEDA complex is tetrameric,<sup>35b</sup> and even in the absence of donor ligands, a tetrameric structure is maintained.<sup>35c</sup> The HMPA titration is straightforward and easy to interpret. Assignments are given in Figure 20. There is a uniform progression of <sup>7</sup>Li and <sup>31</sup>P signals from (MeLi)<sub>4</sub>h<sub>0</sub> to (MeLi)<sub>4</sub>h<sub>1</sub> (with a 1:3 ratio of doublet and singlet Li signals), (MeLi)<sub>4</sub>h<sub>2</sub> (1:1 ratio), (MeLi)<sub>4</sub>h<sub>3</sub> (3:1 ratio), and finally (MeLi)<sub>4</sub>h<sub>4</sub>, a doublet. All signals are resolved. There is no indication of any dissociation to dimers and monomers, only the progressive coordination of the four corners of the methyllithium tetrahedron. Excess HMPA appears at <1 equiv of HMPA, and even at 6 equiv all four sites on the tetramer are not fully occupied by HMPA. This behavior is very similar to that reported for lithium *p*-bromophenoxide.<sup>7</sup>

The experiment was performed on commercial "low-halide" methyllithium. As a result, above 0.5 equiv of HMPA, low-intensity but characteristic signals of Cl-LiH<sub>2</sub> appear, as well as the signals of a separated LiH<sub>4</sub><sup>+</sup> species, which is probably Cl<sup>-</sup>/LiH<sub>4</sub><sup>+</sup>. It is interesting that HMPA selectively extrudes LiCl from what is presumably a mixed aggregate in THF (a crystal structure of such a mixed aggregate with phenyllithium, (PhLi)<sub>3</sub>LiBr, has been reported<sup>31</sup>). This is understandable on thermodynamic grounds: in an HMPA-rich environment the most electrophilic lithium species will selectively be complexed by

(34) Jackman, L. M.; Scarmoutzos, L. M. *J. Am. Chem. Soc.* **1984**, *106*, 4627. Jones, A. J.; Grant, D. M.; Russell, J. G.; Fraenkel, G. *J. Phys. Chem.* **1969**, *73*, 1624.

(35) (a) West, P.; Waack, R. *J. Am. Chem. Soc.* **1967**, *89*, 4395. Köster, H.; Thoennes, D.; Weiss, E. *J. Organomet. Chem.* **1978**, *160*, 1. (c) Weiss, E.; Lucken, E. A. C. *J. Organomet. Chem.* **1964**, *2*, 197.

(30) Bauer, W.; Seebach, D. *Helv. Chim. Acta* **1984**, *67*, 1972.

(31) Hope, H.; Power, P. P. *J. Am. Chem. Soc.* **1983**, *105*, 5320.

(32) Thoennes, D.; Weiss, E. *Chem. Ber.* **1978**, *111*, 3157.

(33) Weiss Schumann, U.; Kopf, J.; Weiss, E. *Angew. Chem., Int. Ed. Engl.* **1985**, *24*, 215.

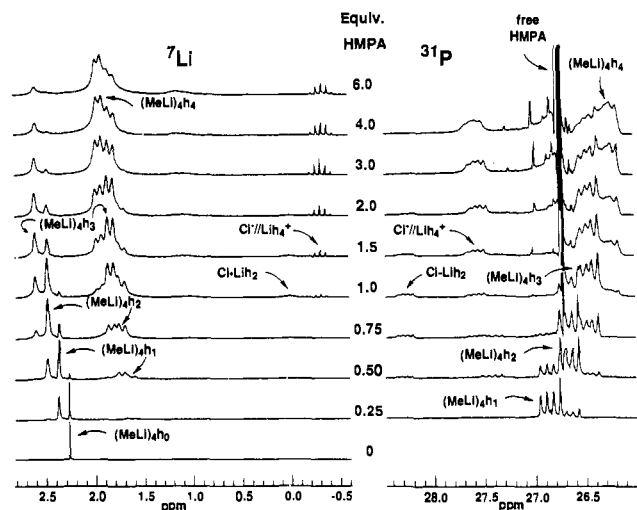


Figure 20. HMPA titration of 0.16 M MeLi in 3:2 THF/ether at  $-135^{\circ}\text{C}$ .

HMPA.<sup>1b</sup> Comparison of the MeLi and LiCl titrations presented in Figures 20 and 18 shows unambiguously that LiCl is considerably more electrophilic than MeLi.

**Distinguishing Contact and Separated Ions in THF.** We have presented HMPA titrations of several systems for which a case can be made that a transition from contact to separated ions occurs as HMPA is added. The key features of contact ions are the following.

(1) Observation of  $^1J_{\text{Li-X}}$  coupling. One-bond coupling between lithium and several other nuclei has been observed, providing preemptory evidence for contact ion pairs. This technique may require the preparation of  $^6\text{Li}$  and/or  $^{13}\text{C}$  or  $^{15}\text{N}$  isotopically enriched compounds. For this paper, we have obtained  $J_{\text{C-X}}$  information for phenyllithium, thus confirming the monomer structure of  $\text{Ph-LiH}_1$ ,<sup>1a</sup> and we have attempted to determine the selenium-lithium coupling in MeSeLi, which gives only a broad singlet in the  $^{77}\text{Se}$  NMR spectrum at the lowest temperatures examined ( $-116^{\circ}\text{C}$ ). We have, however, observed Li-Se coupling in PhSeLi in ether solution, where exchange is slower.<sup>1f</sup> The absence of coupling does not provide useful information.

(2) Deviation of Li and P chemical shifts from the very narrow range found for separated ions. Apart from fluorenyl, which is understandably anomalous, the  $\text{LiH}_0^+$  to  $\text{LiH}_4^+$  signals are identical for all separated ions to within 0.2 ppm in the Li and P spectra. This criterion is complicated by the problems of external chemical shift referencing.

(3) Concentration of  $\text{LiH}_n^+$  species during the titration. In every case examined except for LiI, the process of ion separation is accompanied by a sudden jump in the HMPA coordination (e.g.,  $\text{Br-LiH}_1$  contact going to  $\text{Br}^-//\text{LiH}_3^+$  separated, with only a low concentration of  $\text{Br-LiH}_2$  contact).

(4) Early appearance of free HMPA. For very difficult to separate ions and those that form stable aggregates, the appearance early in the titration of free HMPA, sometimes in dynamic exchange with coordinated HMPA, is very characteristic. Such species may not form significant amounts of separated ions even when a large excess of HMPA is present. Specifically, localized carbanions (e.g., methyllithium, phenyllithium, lithium acetylides), alkoxides,<sup>7</sup> and lithium amides<sup>6</sup> behave in this way.

Figure 21 presents a stacked plot of several lithium reagents at 1 equiv of HMPA, and Figure 22 a similar set at 2 equiv. In each case, the spectra are ordered by ease of ionization, with the bottom spectra being the separated ion pair, lithium triphenylmethide, and the top spectra being the relatively hard to ionize lithium methanethiolate. The analysis and assignments have been made earlier. These comparisons point out the simplicity of separated ions compared to contact monomers, as well as the

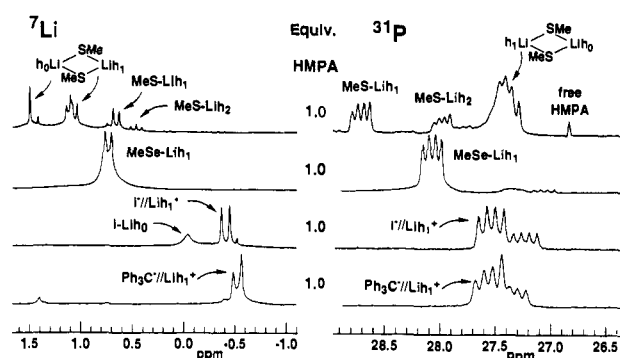


Figure 21.  $^7\text{Li}$  and  $^{31}\text{P}$  NMR spectra of 2Li, LiI, MeSeLi, and MeSLi at 1.0 equiv of HMPA.

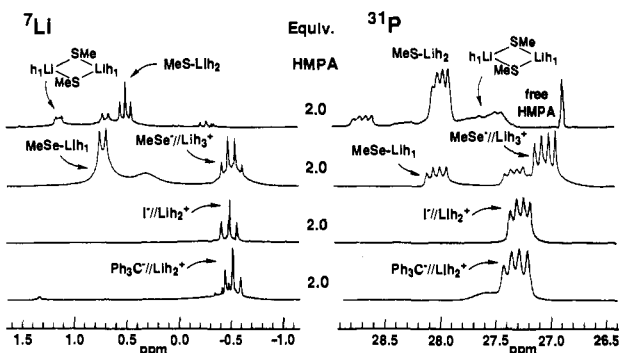


Figure 22.  $^7\text{Li}$  and  $^{31}\text{P}$  NMR spectra of 2Li, LiI, MeSeLi, and MeSLi at 2.0 equiv of HMPA.

further increase in complexity when aggregation occurs. It also illustrates the disproportionation effect when ion separation occurs: at 2 equiv of HMPA (Figure 22), MeSeLi shows mono and tris HMPA complexed lithium, whereas the separated ions show only the bis complex. Finally, only strongly coordinated ion pairs (such as MeSLi) show free HMPA early in the titration.

**General Comments about the HMPA Titration Technique.** We have illustrated here and in previous papers<sup>1b,e</sup> that ion pair structure in THF can be easily determined by doing a very low temperature HMPA titration monitored by  $^7\text{Li}$  (or  $^6\text{Li}$ ) and  $^{31}\text{P}$  NMR, as well as other appropriate nuclei. It is *mandatory* to observe  $^{31}\text{P}$  coupling. Without this, the confident assignment of signals to individual ions is difficult or impossible. We found that some solutions made from scrupulously dried lithium salts (e.g., lithium halides) do not give sharp lines at low temperatures. In these cases addition of a small amount (5–10%) of an organolithium reagent seems to remove trace protic impurities (probably water) which catalyze exchange of HMPA between lithium cations.

It generally appears to be true for contact ions that the higher HMPA solvates undergo the most rapid dynamic exchange and give the broadest lines. We, therefore, have observed many examples of the  $\text{CIP R-LiH}_1$  and several cases of  $\text{R-LiH}_2$ , but we have never observed the  $\text{CIP R-LiH}_3$  as a distinct species. This is presumably because each coordinated HMPA reduces the electrophilicity of the lithium such that exchange between free and bound HMPA becomes progressively faster until the rate is too fast to allow the individual detection of contact  $\text{R-LiH}_3$  (and in some cases,  $\text{R-LiH}_2$  at all but extremely low temperatures) by our NMR technique. It is also likely that sometimes the formation constant of these complexes is unfavorable. In contrast, for separated ions, the higher solvates  $\text{R}^-//\text{LiH}_3^+$  and  $\text{R}^-//\text{LiH}_4^+$  undergo slower exchange with each other and with free HMPA than do  $\text{R}^-//\text{LiH}_1^+$  and  $\text{R}^-//\text{LiH}_2^+$ .

**Execution of HMPA Titrations.** One of the more attractive features of our technique is the relative ease with which the samples can be prepared and the titration carried out. Generally, the

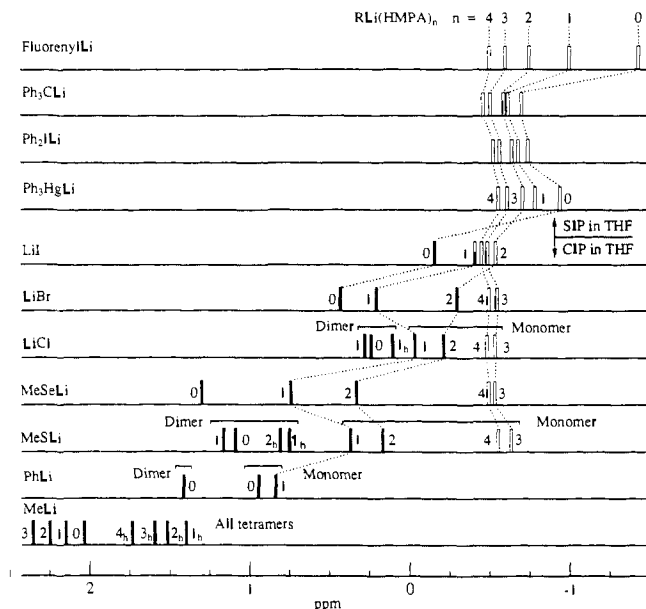


**Figure 23.**  ${}^7\text{Li}$  chemical shifts of  $\text{RLi}(\text{HMPA})_n$ . Open bars are SIPs; solid, CIPs. Those shifts which were measured in 3:2 THF/ether (LiCl, MeSLi, MeLi) were moved 0.25 ppm upfield to correct for the solvent change.

lithium reagent is prepared in a septum-capped 10-mm NMR tube by metalation, Li/X exchange, or some other reaction with MeLi, *n*-BuLi, or PhLi. This solution is titrated by the syringe addition of aliquots of HMPA. While more rigorous vacuum line techniques may provide a scrupulously oxygen-free and dry system, those techniques are generally tedious and would require the preparation of eight or nine samples for a typical titration. On the other hand, the technique we use requires the preparation of a single sample for a complete titration. Of the dozens of systems which we have looked at in some detail, we have encountered little difficulty in maintaining a dry system, and in general we have obtained good yields of the quenched lithium reagent. The main source of difficulty is reactive lithium reagents which decompose upon addition of HMPA. Of course, this would be the case regardless of how the lithium reagent was prepared or titrated.

**Donor Strength of Anionic Ligands.** The results presented here (and some previously published and unpublished data) show that HMPA is able to displace all of the anions investigated except for  $\text{Me}^-$  and  $\text{Ph}^-$  from lithium. We can therefore postulate the following sequence of donor strengths toward  $\text{Li}^+$  from our data:  $\text{Me}^-$ ,  $\text{Ph}^- > \text{HMPA} > \text{Cl}^-$ ,  $\text{MeS}^- > \text{Br}^-$ ,  $\text{MeSe}^- > \text{I}^- > \text{THF} > \text{Ph}_3\text{Hg}^- \approx \text{fluorenyl anion} \approx \text{trityl anion} > \text{ether}$ . Our results can be compared to those obtained by Collum and co-workers for lithium amides<sup>6</sup> and Jackman and co-workers for lithium alkoxides.<sup>7</sup> These workers found that HMPA does not effectively break up dimeric amides or phenoxides, or tetrameric unhindered phenoxides, and in fact may actually increase average aggregation state. Furthermore, little or no ion separation occurs. We conclude, therefore, that to a first approximation the donor strength of  $\text{RO}^-$ ,  $\text{R}_2\text{N}^-$ , and even lithium-coordinated alkoxide or amide is greater than or comparable to HMPA. Hence  $\text{RO}^- > \text{ROLi} \approx \text{HMPA} > \text{THF}$  and  $\text{R}_2\text{N}^- > \text{R}_2\text{NLi} \approx \text{HMPA} > \text{THF}$  (where R is a simple alkyl group). It is clear that the strength of coordination of an anion to  $\text{Li}^+$  is only marginally related to  $\text{p}K_a$ , but is profoundly influenced by charge delocalization, either by means of conjugation (trityl and fluorenyl vs phenyl) or the size of the anionic center (chloride or methylmercaptide vs iodide).

**Summary of Lithium and Phosphorus Chemical Shifts and Couplings.** The chemical shifts of the different species in the lithium and phosphorus spectra are presented in Figures 23 and

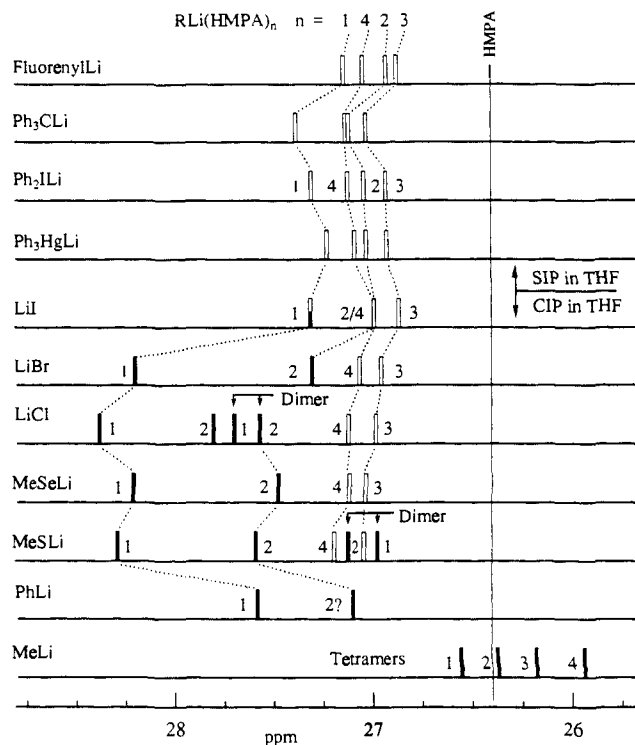


**Figure 24.**  ${}^{31}\text{P}$  chemical shifts of  $\text{RLi}(\text{HMPA})_n$ . Open bars are SIPs; solid, CIPs. Those shifts which were measured in 3:2 THF/ether (LiCl, MeSLi) were moved  $\approx 0.3$  ppm upfield to correct for the solvent change.

24, respectively. The open bars have been identified as separated ions and the closed bars as contact ions. Since external referencing was used and some of the compounds were measured in pure THF and others in 3:2 THF/ether, we have applied a chemical shift correction of  $\approx 0.3$  ppm to the latter (this value was estimated from the chemical shift of free HMPA and from the shift of identical separated ions in the two media). The graphical format illustrates that the chemical shifts are quite invariant for separated ions  $\text{Li}h_n^+$  when  $n = 3$  or 4 (the small variations are probably within experimental error because of referencing uncertainties). For contact ions, diverse shifts are obtained. The graphs illustrate that for most systems chemical shift alone can provide a good basis for distinguishing contact and separated ions, especially for the  ${}^7\text{Li}$  nucleus. With the lone exception of lithium fluorenyl in ether, all contact lithium shifts are downfield of the separated ions (this is true also for several dozen other ions that we have studied, including many carbanions). The  ${}^{31}\text{P}$  shifts are not very consistent. For the compounds studied in this paper we have observed mostly downfield shifts for coordinated vs free HMPA, with methyl lithium the lone exception. However, if a broader variety of ions is examined, upfield shifts are quite common (e.g., contact silyl-substituted carbanions usually have  $\text{RLi}h_1$  upfield of HMPA<sup>1e</sup>).

Table I presents the Li-P coupling constants for the systems discussed in this paper. The couplings all fall in a narrow range of 7.4–11.5 Hz, with the smallest values observed for separated  $\text{Li}h_4^+$  and the largest for separated  $\text{Li}h_1^+$ . HMPA complexes of lithium phenoxides<sup>5b,7</sup> and lithium amides<sup>6</sup> also fall in this range, irrespective of the degree of aggregation. Much smaller couplings (3.8 Hz) have been observed when HMPA bridges two lithium cations.<sup>1f,5a</sup>

**Summary.** The effects of HMPA on solutions of organolithium species is diverse. In all cases examined, at least one HMPA coordinates strongly to the lithium. Additional equivalents of HMPA may not coordinate detectably (as for MeLi), may coordinate weakly (PhLi), may cause deaggregation of dimers to monomers (MeSLi and LiCl), may coordinate a second HMPA while maintaining a contact ion structure (MeSeLi and LiBr),

Table I. Lithium-Phosphorus Coupling Constants ( $^2J_{\text{Li-P}}$ )

| species              | <i>n</i><br>(HMPA) | $^2J_{\text{Li-P}}$<br>(Hz) | species | <i>n</i><br>(HMPA) | $^2J_{\text{Li-P}}$<br>(Hz) |
|----------------------|--------------------|-----------------------------|---------|--------------------|-----------------------------|
| PhLi                 | 1-SIP              | 11.1                        | LiBr    | 1-CIP              | 8.8                         |
|                      | 2-SIP              | 10.7                        |         | 2-CIP              | 8.9                         |
|                      | 3-SIP              | 9.3                         |         | 3-SIP              | 9.3                         |
|                      | 4-SIP              | 7.7                         |         | 4-SIP              | 7.7                         |
| Ph <sub>3</sub> CLi  | 1-SIP              | 11.6                        | LiI     | 1-S/C <sup>a</sup> | 11.3                        |
|                      | 2-SIP              | 10.4                        |         | 2-SIP              | 10.4                        |
|                      | 3-SIP              | 9.2                         |         | 3-SIP              | 9.3                         |
|                      | 4-SIP              | 7.6                         |         | 4-SIP              | 7.6                         |
| Ph <sub>2</sub> ILi  | 1-SIP              | 11.3                        | MeSeLi  | 1-CIP              | 8.6                         |
|                      | 2-SIP              | 10.4                        |         | 2-CIP              | 8.2                         |
|                      | 3-SIP              | 9.1                         |         | 3-SIP              | 9.4                         |
|                      | 4-SIP              | 7.5                         |         | 4-SIP              | 7.5                         |
| Ph <sub>3</sub> HgLi | 1-SIP              | 11.8                        | MeLi    | 1-tet <sup>b</sup> | 9.9                         |
|                      | 2-SIP              | 10.2                        |         | 2-tet              | 9.1                         |
|                      | 3-SIP              | 9.2                         |         | 3-tet              | 8.5                         |
|                      | 4-SIP              | 7.6                         |         | 4-tet              | 7.7                         |
| LiCl                 | 1-dimer            | 9.4                         | MeSLi   | 1-dimer            | 8.7                         |
|                      | 2-dimer            | 9.6                         |         | 2-dimer            | 8.0                         |
|                      | 1-CIP              | 8.1                         |         | 1-CIP              | 7.9                         |
|                      | 2-CIP              | 7.6                         |         | 2-CIP              | 7.3                         |
|                      | 3-SIP              | 9.7                         |         | 3-SIP              | 9.3                         |
|                      | 4-SIP              | 7.7                         |         | 4-SIP              | 7.5                         |

<sup>a</sup> This species seems to be a mixture of contact and separated ions.

<sup>b</sup> All of the MeLi species are tetramers.

or may coordinate and cause ion separation (MeSeLi, LiBr, LiI). With an excess of HMPA, MeLi remains a tetramer and PhLi remains a monomer, whereas MeSLi, MeSeLi, LiI, LiBr, and LiCl all form separated ions. These data provide a rational basis for understanding the powerful activating effects of HMPA on these and other lithium species.

### Experimental Section

**General.** Glassware was dried overnight in a 110 °C oven or flame dried to remove moisture. Common lithium reagents were titrated with *n*-PrOH in ether or THF using 1,10-phenanthroline as indicator. Tetrahydrofuran (THF) and ether were freshly distilled from sodium benzophenone ketyl before use. Hexamethylphosphoric triamide (HMPA) was obtained from Aldrich, distilled from CaH<sub>2</sub>, and stored under N<sub>2</sub> over molecular sieves. Transfer of HMPA were done by syringe techniques in a fume hood. HMPA is a suspected carcinogen,<sup>36</sup> and adequate precautions must be taken to avoid all forms of exposure.

Starting materials were commercially available except for compounds referenced in the experimental sections. Reported reaction temperatures are those of the cooling bath, with -78 °C being maintained by a dry ice/ethanol bath.

**Preparation of Salt-Free PhLi.**<sup>27,37</sup> A 250-mL three-neck round-bottom flask equipped with a stir bar and a modified side arm which contained a glass frit, a stopcock, and a 14/35 joint was dried and flushed with N<sub>2</sub>, and PhI (22.4 g, 110 mmol, 12.3 mL) and 20 mL of N<sub>2</sub>-sparged hexane were added. *n*-BuLi (101 mmol, 57.0 mL, 1.77 M in hexane) was added over 30 min to the stirred and ice water cooled solution. PhLi immediately precipitated, and the mixture was stirred for an additional 40 min. (Since the precipitated PhLi makes magnetic stirring difficult, an additional 75–100 mL of hexane can be added to the flask.) The mixture was filtered through the glass frit with the aid of a vacuum (~0.1 mmHg). The off-white cake of PhLi was broken up by shaking the flask, and the powder was washed with 100 mL of pentane (N<sub>2</sub> sparged), stirred for a few minutes, and filtered through the glass frit. This process was repeated three more times. The solid cake was broken up by shaking and was placed under vacuum for ~45 min. Enough freshly distilled ether was added to give about 50 mL of solution (warming!), and the solution was transferred by cannula to two dry, N<sub>2</sub>-flushed 50-mL Erlenmeyer flasks with 24/40 joints and septa. These were placed in the freezer overnight (-25 °C). PhLi crystals formed, and the supernatant was removed by

cannula. PhLi was recrystallized twice from ether. The supernatant was removed by cannula, and ether was added to make an ethereal solution of PhLi (2.91 M). To an N<sub>2</sub>-flushed, dry 10-mm NMR tube was added 3.8 mL of freshly distilled THF at -78 °C, and PhLi (0.11 mL, 0.32 mmol, 2.91 M in ether) was added to give ~0.08 M solution in THF. <sup>7</sup>Li NMR of the solution at -120 °C showed that the PhLi was clean with the exception of a small impurity at  $\delta$  0.88. (The chemical shift of the PhLi monomer is  $\delta$  0.95, and that of the PhLi dimer is  $\delta$  1.42.) For long-term storage the PhLi was stored in ether.

PhLi in THF was formed by cooling the ethereal PhLi solution to -78 °C, removing the supernatant ether, and adding enough dry THF to dissolve the crystalline PhLi. Crystals were formed upon cooling in the freezer, and the flask was further cooled with dry ice. The THF was removed by cannula, and THF was added to give PhLi (THF). The molarity was determined to be 1.34 M by titration, as above.

**Preparation of *n*-Bu<sup>6</sup>Li.**<sup>10,11b</sup> A block of <sup>6</sup>Li<sup>o</sup> (7.6 g, 1.3 mol) was washed with hexane and placed in a glovebag that was inflated with N<sub>2</sub>. The oxide was scraped off, and the <sup>6</sup>Li<sup>o</sup> was cut into small pieces using scissors and forceps. The <sup>6</sup>Li<sup>o</sup> was transferred into a 500-mL round-bottom flask in the glovebag; the flask was fitted with a 24/40 septum, and the flask was removed. The flask was briefly flushed with N<sub>2</sub>. (Note: During the short period of flushing the flask became too hot to touch). Apparently the fresh Li<sup>o</sup> surface was reacting with N<sub>2</sub> to form lithium nitride (Li<sub>3</sub>N).) Degassed hexane (250 mL) and *n*-BuCl (53 mL, 46.9 g, 0.51 mol) were added to the flask; within 10 min the solution was warm and turning gray. The mixture was stirred for 1 week, a red precipitate formed, and then a gelatinous substance was allowed to settle for a day. About 4 in. of oven-dried Celite was placed in a 6-in. filter funnel. The reaction flask was attached to the filter funnel by a large bore cannula, and the filter funnel was connected to a small vessel which was connected by cannula to a 500-mL round-bottom flask. The receiving flask was cooled in a -78 °C bath and attached to a pump to aid in the filtration of the hexane solution of *n*-Bu<sup>6</sup>Li. The mixture was transferred to the Celite (there were losses due to the gelatinous precipitate. The plug of Celite was rinsed with 100–150 mL of degassed pentane until the yellow color on the Celite disappeared, and the receiving flask was warmed under vacuum until the volume had been reduced to about 30 mL. The *n*-Bu<sup>6</sup>Li was titrated to be 5.96 M. About 30 mL of degassed hexane was added, and the solution was transferred by cannula to a 125-mL Erlenmeyer flask with a 24/40 joint. This solution was 2.75 M by titration and was stored in the freezer under a positive N<sub>2</sub> pressure.

**NMR Spectroscopy.** <sup>1</sup>H nuclear magnetic resonance (NMR) spectra were obtained on Bruker WP-200 or WP-270 spectrometers. All <sup>1</sup>H NMR spectra were measured in CDCl<sub>3</sub> with tetramethylsilane (TMS) as an internal standard ( $\delta$  0.00).

All multinuclear low-temperature NMR experiments were run on a wide-bore AM-360 spectrometer at 139.962 MHz (<sup>7</sup>Li), 52.998 MHz (<sup>6</sup>Li), 145.784 MHz (<sup>31</sup>P), or 90.56 MHz (<sup>13</sup>C) with the spectrometer unlocked. Digital resolution was 0.5–1.0 Hz for <sup>7</sup>Li and 0.6–1.2 Hz for <sup>31</sup>P. For a 0.15 M solution, 40 transients for the <sup>7</sup>Li spectrum and 80–120 scans for the <sup>31</sup>P spectrum afforded an excellent signal to noise ratio. (Note: Although the spectrometer was unlocked during acquisition, the field was generally very stable and only occasionally did an experiment have to be abandoned due to a field shift.)

Gaussian multiplication (GM) was performed using the Gaussian broadening parameter (GB) equal to the duration of the FID and the line-broadening parameter (LB) equal to -(digital resolution)/GB.

**General Procedure for HMPA Titration of Lithium Reagents.** Samples of the lithium reagent (0.66 mmol) in THF or other solvent (3.5 mL) were prepared in 10-mm thin-walled NMR tubes, which were N<sub>2</sub> flushed, oven-dried, and fitted with a septum (9-mm i.d.). The outside top portion of the tube was lightly greased to make a better seal for the septa, which were held securely by parafilm. Silicon grease was placed on the septa tops to seal punctures, and the tubes were stored at -78 °C until the experiment was performed. After we adjusted the shim values for the CDCl<sub>3</sub> lock sample, the AM-360 spectrometer was unlocked, the probe was cooled (-120 to -130 °C), and the temperature was measured before and after the experiment using a calibrated RTD (resistance temperature device) accurate to 0.03 °C. The reading was taken 10–15 min after the RTD element had been lowered into the probe. (The reading fluctuated within ~0.1 °C at this point.) The sample was inserted and the spectrometer tuned. Since deuterated solvents were not used, the field was tuned on the <sup>13</sup>C FID of C-3 of THF, and NMR spectra of <sup>7</sup>Li, <sup>31</sup>P, and other nuclei were measured. The sample was ejected, placed in a -78 °C bath, and for example, 0.25 equiv of HMPA (28.0  $\mu$ L, 0.161

(36) Mihal, C. P., Jr. *Am. Ind. Hyg. Assoc. J.* 1987, 48, 997. American Conference of Governmental Industrial Hygienists: *TLVs—Threshold Limit Values and Biological Exposure Indices for 1986–1987*; ACGIH: Cincinnati, OH, Appendix A2, p 40.

(37) Several procedures have been used to prepare salt-free phenyllithium: Waack, R.; Doran, M. A. *Chem. Ind. (London)* 1964, 12, 496. Schlosser, M. *J. Organomet. Chem.* 1967, 8, 193.

mmol, 28.8 mg) was added. In order to get the HMPA to dissolve, the tube had to be repeatedly warmed slightly and shaken. The sample was placed in the probe, and after about 10 min the  $^7\text{Li}$  and  $^{31}\text{P}$  NMR spectra were taken. Spectra were typically taken at 0, 0.25, 0.5, 1.0, 2.0, 3.0, 4.0, 6.0, and 10.0 equiv of HMPA.

**Referencing  $^7\text{Li}$  and  $^{31}\text{P}$  NMR Spectra.** The  $^7\text{Li}$  and  $^{31}\text{P}$  chemical shift references were sealed capillary tubes containing  $\text{LiCl}$  (0.3 M  $\text{MeOH}$ ,  $\delta$  0.00) and  $\text{PPh}_3$  (1 M  $\text{THF}$ ,  $\delta$  -6.00), respectively. These tubes were oven-dried before use. Referencing was done at the temperature of the experiment, unless this was too low (the reference samples froze at  $\approx -125$  °C). Referencing throughout the experiment was not feasible because the capillary samples caused lower spectrum quality and obscured some of the signals. Two general referencing techniques were used.

**Procedure A:** Two samples of the lithium reagent were prepared, the  $^7\text{Li}$  and  $^{31}\text{P}$  references were placed in one of the tubes, and parallel titrations were performed. The reference sample was not usually carried through the entire titration. With procedure A accurate referencing can be achieved. However, ultralow temperature experiments cannot be carried out with capillary tubes present since they promote sample crystallization and the references freeze. It is also difficult to dissolve frozen HMPA by shaking NMR tubes containing reference tubes.

**Procedure B:** The problems noted above can be circumvented by the following procedure. At the conclusion of the experiment, the septum was removed under a stream of nitrogen, the chemical shift references were inserted, and the septum was replaced. The chemical shifts of the HMPA species present were measured and used to reference earlier spectra in the titration. An important advantage for valuable samples is that only one sample needs to be prepared.

Under these conditions, with THF as the solvent, free HMPA appeared at  $\delta$  26.4, the  $\text{LiH}_4^{+31}\text{P}$  signal at  $\delta$  27.1, and the Li quintet at  $\delta$  -0.5. In 3:2 THF/ether, HMPA appeared at  $\delta$  26.6, the  $\text{LiH}_4^{+31}\text{P}$  signal at  $\delta$  27.3, and the Li quintet at  $\delta$  -0.3. Independent of the method used, there are unavoidable referencing errors (temperature dependent  $\delta$ , differences in solvent composition resulting from methods used to prepare the samples, spectrometer drift) which could result in errors of at least 0.1 ppm.

**$^7\text{Li}$  and  $^{31}\text{P}$  NMR Spectroscopy of an HMPA Titration of Fluorenyllithium (1Li) in THF (Figure 1).** To oven-dried NMR tubes were added 109 mg (0.660 mmol) of fluorene and 3.8 mL of THF. The tubes were cooled to 0 °C, and *n*-BuLi (0.22 mL, 0.64 mmol, 2.91 M) was added, which almost immediately generated an orange solution. While we ensured a positive pressure of  $\text{N}_2$  during the metalation, the tubes were transferred to a -78 °C bath, and the experiment was performed. Procedure A was used for referencing, and the fluorenyllithium signal was set to  $\delta$  -1.44. The probe temperature drifted from -124.6 to -125.6 °C during the titration.

The sample was quenched with MeI (80  $\mu\text{L}$ , 0.18 g, 1.3 mmol), allowed to warm to room temperature, and poured into water and 1:1 ether/pentane. The organic phase was extracted several times with water and once with brine and dried ( $\text{Na}_2\text{SO}_4$ ), and the solvents were evaporated to yield an oil. Pentachloroethane (NMR standard, 75.0  $\mu\text{L}$ , 0.625 mmol, 0.126 g) and  $\text{CDCl}_3$  were added to the oil. A 200-MHz  $^1\text{H}$  NMR spectrum (recycle delay of 10.0 s) showed a 91% yield of 9-methylfluorene.

**Variable Temperature  $^7\text{Li}$  and  $^{31}\text{P}$  NMR Spectroscopy of 0.04 and 0.16 M Fluorenyllithium (1Li) at 0.5 equiv of HMPA in THF (Figure 2).** Samples of 0.04 and 0.16 M 1Li were prepared in 10-mm NMR tubes as in the procedure above. Low-temperature  $^7\text{Li}$  spectra were taken of the two samples to confirm purity, HMPA (0.5 equiv) was added to both samples, and the variable temperature experiments was begun. The order of events was temperature measurement, acquisition of  $^7\text{Li}$  and  $^{31}\text{P}$  spectra of the 0.04 M sample, acquisition of  $^7\text{Li}$  and  $^{31}\text{P}$  of the 0.16 M sample, and then a second temperature measurement. The two temperatures differed at most by 1°, and usually less than 0.5°. MeI quench gave a 78% yield of 9-methylfluorene (89% based on *n*-BuLi added) and 19% of fluorene for the 0.04 M sample, and a 95% yield of 9-methylfluorene (97% based on *n*-BuLi) and 3% fluorene for the 0.16 M sample.

**Variable Temperature  $^7\text{Li}$  and  $^{31}\text{P}$  NMR Spectroscopy of 0.04 and 0.16 M Fluorenyllithium (1Li) at 4.0 equiv of HMPA in THF (Figure 3).** Samples were prepared as above except that HMPA (4.0 equiv) was added to both samples. MeI quench of the samples gave an 87% yield of 9-methylfluorene (92% based on *n*-BuLi added) and 10% fluorene for the 0.04 M sample, and an 87% yield of 9-methylfluorene (98% based on *n*-BuLi) and 8% of fluorene for the 0.16 M sample.

**$^7\text{Li}$  and  $^{31}\text{P}$  NMR Spectroscopy of an HMPA Titration of Fluorenyllithium (1Li) in Ether (Figure 6).** The procedure is that of 1Li except that ether was used as solvent and metalation was carried out at -78 °C overnight. Referencing was by procedure A,  $^{31}\text{P}$  spectra were taken at

0.0, 0.125, 0.25, 0.5, 1.0, 1.5, and 2.0 equiv of HMPA. A few white crystals were present at 1.0 equiv of HMPA. At 1.5 and 2.0 equiv of HMPA, the precipitate had a depth of about 5 and 8 mm, respectively, in the NMR tube. At 3 equiv of HMPA, no Li or P NMR signals were detectable. The temperature of the probe before the experiment was -120.5 °C; after the experiment it was -122.4 °C. The sample was quenched with MeI, THF was added (the reaction was slow in ether), and NMR analysis revealed a 97% yield of 9-methylfluorene.

**$^7\text{Li}$  and  $^{31}\text{P}$  NMR Spectroscopy of an HMPA Titration of Trityllithium (2Li) in 3:2 THF/Ether (Figure 7).** To a 10-mm NMR tube containing  $\text{Ph}_3\text{CH}$  (0.171 g, 0.70 mmol) in 2.1 mL of THF cooled to -78 °C was added MeLi (0.463 mL, 0.70 mmol, 1.51 M in ether), followed by an additional 0.94 mL of  $\text{Et}_2\text{O}$  to give a total solvent volume of 3.5 mL. As the metalation proceeded, the solution turned pink and finally deep red upon storing at -20 °C (freezer temperature) for 18 h.  $^7\text{Li}$  and  $^{31}\text{P}$  spectra were taken at 0, 0.4, 0.8, 1.2, 1.6, 2.0, 3.0, 4.0, and 6.0 equiv of HMPA. The temperature of the probe during the experiment was -128 °C. NMR analysis of MeI-quenched lithium reagent gave an 83% yield of  $\text{Ph}_3\text{CCH}_3$  and a 17% yield of  $\text{Ph}_3\text{CH}$ . The metalation of  $\text{Ph}_3\text{CH}$  with MeLi (or *n*-BuLi) was incomplete since both MeLi and  $\text{Ph}_3\text{CH}$  were present at the beginning of the titration, and only by 6.0 equiv of HMPA was reaction complete.

**$^7\text{Li}$  and  $^{31}\text{P}$  NMR Spectroscopy of an HMPA Titration of Lithium Triphenylmercuride (3Li) in THF (Figure 8).** The sample was prepared by the reaction of  $\text{Ph}_2\text{Hg}$  (0.218 g, 0.613 mmol) in THF (2.9 mL) with PhLi (0.90 mL, 0.613 mmol, 0.68 M in THF) at -78 °C. The samples were stored overnight. Reference spectra (procedure A) were taken at 0.0, 0.25, and 4.0 equiv of HMPA. The temperature of the probe before the experiment was -122.6 °C; after the experiment it was -117.0 °C. The NMR sample was quenched with 2 equiv of  $\text{Me}_2\text{S}_2$  (110  $\mu\text{L}$ , 1.22 mmol, 115 mg). GC analysis of PhSMe gave an 85% recovery of PhLi.

**$^7\text{Li}$  and  $^{31}\text{P}$  NMR Spectroscopy of an HMPA Titration of LiI in 3:2 THF/Ether (Figure 10).** To a 10-mm NMR tube containing LiI (94 mg, 0.070 mmol) and references were added 2.0 mL of THF, 1.0 mL of ether, and 0.10 equiv of lithium diisopropylamide (0.063 mL, 0.070 mmol, 1.12 M in ether).  $^7\text{Li}$  and  $^{31}\text{P}$  NMR spectra of the reference sample were taken at 0, 0.25, 0.5, 1.5, 2.0, 3.0, 4.0, and 6.0 equiv of HMPA. Good results were also obtained by generating lithium iodide from MeLi and MeI (see below).

**Variable Temperature  $^7\text{Li}$  and  $^{31}\text{P}$  NMR Spectroscopy of LiI at equiv of HMPA in 3:2 THF/Ether (Figure 11).** The sample was prepared by addition of MeLi (0.49 mL, 0.75 mmol, 1.51 M in ether) to a solution of MeI (0.044 mL, 0.70 mmol) in 1.11 mL of ether and 2.4 mL of THF at -78 °C.  $^7\text{Li}$  and  $^{31}\text{P}$  spectra were taken of a sample with 3.0 equiv of HMPA (0.37 mL, 2.1 mmol) at probe temperatures of -135, -125, -115, and -105 °C. Referencing was by procedure B.

**$^7\text{Li}$  and  $^{31}\text{P}$  NMR Spectroscopy of an HMPA Titration of LiBr in 3:2 THF/Ether (Figure 12).** To the 10-mm NMR tube containing dibromoethane (0.035 mL, 0.40 mmol) and 2.4 mL of THF cooled to -78 °C was added 2 equiv of MeLi (0.53 mL, 0.80 mmol, 1.51 M in ether). A colorless precipitate was dissolved upon shaking, and 1.07 mL of ether was added. Only two new signals were observed in the  $^{13}\text{C}$  NMR corresponding to the chemical shifts of ethylene ( $\delta$  126.7) and ethane ( $\delta$  7.6). The  $^7\text{Li}$  and  $^{31}\text{P}$  NMR spectra were taken at 0, 0.25, 0.5, 1.5, 2.0, 3.0, 4.0, and 6.0 equiv of HMPA. The temperature of the probe during the experiment was approximately -130 °C.

Similar results were obtained with commercial LiBr using the following precautions to remove traces of protic impurities (see Figure 9). A 25-mL flask containing 0.5 g of LiBr under high vacuum (<0.005 mm) was gently heated until the LiBr powder no longer "hopped about" as water evaporated, the LiBr was heated until molten, and the flask was allowed to cool under an  $\text{N}_2$  atmosphere. Enough THF was added to give a 1.0 M LiBr solution. As seen in Figure 9, even these vigorous drying conditions were not enough to remove all protic impurities, and it was necessary to add 10% PhLi to the LiBr/THF solution.

**$^7\text{Li}$  and  $^{31}\text{P}$  NMR Spectroscopy of an HMPA Titration of MeSeLi in THF (Figure 13).** A THF solution of  $\text{Me}_2\text{Se}_2$  (60.0  $\mu\text{L}$ , 0.120 g, 0.638 mmol) was cooled to -78 °C, and *n*-BuLi (0.21 mL, 0.636 mmol, 3.03 M in hexane) was added at -78 °C. Reference spectra (procedure A) were taken at 0.0, 0.25, and 4.0 equiv of HMPA. The temperature of the probe before the experiment was -124.4 °C; after the experiment it was -128.8 °C. Benzyl bromide (76.0  $\mu\text{L}$ , 0.109 g, 0.639 mmol) was added to the sample. NMR analysis of the quenched lithium reagent gave a 90% yield of benzyl methyl selenide. The procedure for obtaining the required resolution for MeSe-LiH<sub>2</sub> (Figure 13 inset, 3.0 equiv of HMPA) is as follows. To the 10-mm NMR tube containing dimethyl

diselenide (0.066 mL, 0.70 mmol) in 2.4 mL of THF cooled to  $-78\text{ }^{\circ}\text{C}$  was added MeLi (0.440 mL, 0.70 mmol, 1.59 M in ether), followed by an additional 1.16 mL of ether to give a total solvent volume of 4.0 mL. The colorless samples was stored overnight at  $-78\text{ }^{\circ}\text{C}$ . The temperature of the probe during the experiment was  $-141\text{ }^{\circ}\text{C}$ .  $^7\text{Li}$  and  $^{31}\text{P}$  spectra were taken with probe temperatures of  $-141\text{ }^{\circ}\text{C}$  and  $-121\text{ }^{\circ}\text{C}$  for data on lithium iodide temperature dependence (Figure 11).

**$^7\text{Li}$  and  $^{31}\text{P}$  NMR Spectroscopy of an HMPA Titration of MeSeLi in 3:2 THF/Ether (Figure 14).** To the 10-mm NMR tube containing  $\text{Me}_2\text{S}_2$  (0.044 mL, 0.70 mmol) in 2.6 mL of THF cooled to  $-78\text{ }^{\circ}\text{C}$  was added MeLi (0.464 mL, 0.70 mmol, 1.51 M in ether). Precipitate was formed which was easily dissolved by mixing the solution. An additional 1.34 mL of ether was added to the colorless solution. If the MeSLi was initially formed in 3:2 THF/ $\text{Et}_2\text{O}$ , the precipitate was very difficult to dissolve, even at room temperature. The sample was used immediately with a probe temperature of  $-138\text{ }^{\circ}\text{C}$ . Referencing was done using procedure B.

**Variable Concentration  $^7\text{Li}$  and  $^{31}\text{P}$  NMR Spectroscopy of MeSLi at 1.0 equiv of HMPA in 3:2 THF/Ether (Figure 17).** To a 10-mm NMR tube containing  $\text{Me}_2\text{S}_2$  (0.174 mL, 2.80 mmol) in 2.6 mL of THF cooled to  $-78\text{ }^{\circ}\text{C}$  were added MeLi (1.85 mL, 2.80 mmol, 1.51 M in ether) and 1.0 equiv of HMPA (0.487 mL, 2.80 mmol). A precipitate was formed, which dissolved upon mixing.  $^7\text{Li}$  spectra were taken with a probe temperature of  $-138\text{ }^{\circ}\text{C}$ . The 0.64 M sample was diluted to 0.16 M by twice repeating the process of removing by cannula one-half of the solution volume and replacing with an equal amount of THF/ether (2.60 mL/1.85 mL). Such dilutions were repeated to generate 0.04, 0.01, and 0.002 M solutions of MeSLi.

**$^6\text{Li}$  and  $^{31}\text{P}$  NMR Spectroscopy of an HMPA Titration of Me $^6\text{Li}$  in THF (Figure 15).** The procedure is as above with the following exceptions. To the THF solution of  $\text{Me}_2\text{S}_2$  was added *n*-Bu $^6\text{Li}$  (0.22 mL, 0.631 mmol, 2.87 M in hexane). No reference spectra were taken. The temperature of the probe before the experiment was  $-124.1\text{ }^{\circ}\text{C}$ ; after the experiment it was  $-123.7\text{ }^{\circ}\text{C}$ . Benzyl bromide (76.0  $\mu\text{L}$ , 0.109 g, 0.639 mmol) was added to the sample. NMR analysis of the quenched lithium reagent gave a 98% yield of benzyl methyl sulfide.

**Variable Concentration  $^7\text{Li}$  and  $^{31}\text{P}$  NMR Spectroscopy of LiCl at 1.0 equiv of HMPA in 3:2 THF/Ether (Figure 17).** To a 10-mm NMR tube containing LiCl (0.174 mL, 2.80 mmol) was added 2.40 mL of THF, and the mixture was shaken to form a homogeneous solution. Ether (1.60 mL), LDA (0.10 equiv, 0.125 mL, 0.14 mmol, 1.12 M), and 1.0 equiv

of HMPA (0.122 mL, 0.70 mmol) were added.  $^7\text{Li}$  spectra were taken of the sample with a probe temperature of  $-142\text{ }^{\circ}\text{C}$ . The 0.16 M sample was diluted as described above to generate 0.08, 0.04, and 0.01 M solutions. Solutions of higher molarity could not be generated due to the insolubility of lithium chloride under these conditions.

**$^7\text{Li}$  and  $^{31}\text{P}$  NMR Spectroscopy of an HMPA Titration of LiCl in 3:2 THF/Ether (Figure 18).** To a 10-mm NMR tube containing LiCl (0.021 mg, 0.50 mmol) was added 2.1 mL of THF, and the mixture was shaken to form a homogeneous solution. Ether (1.4 mL) and LDA (0.10 equiv, 0.045 mL, 0.050 mmol, 1.12 M in ether) were added. The temperature of the probe during the experiment was  $-142\text{ }^{\circ}\text{C}$ . Referencing was done using procedure B.

**$^7\text{Li}$  and  $^{31}\text{P}$  NMR Spectroscopy of an HMPA Titration of LiCl in 1:1 THF/ $\text{Me}_2\text{O}$  (Figure 18).** Into a 10-mm NMR tube cooled to  $-78\text{ }^{\circ}\text{C}$  was condensed  $\text{Me}_2\text{O}$  (2 mL), followed by the addition of  $\text{Me}_3\text{SiCl}$  (0.025 mL, 0.20 mmol), MeLi (0.164 mL, 0.25 mmol, 1.52 M in ether), and THF (2.0 mL).  $^7\text{Li}$  and  $^{31}\text{P}$  spectra were taken with a probe temperature of  $-144\text{ }^{\circ}\text{C}$ . Referencing was by procedure B.

**$^7\text{Li}$  and  $^{31}\text{P}$  NMR Spectroscopy of an HMPA Titration of PhLi in THF (Figure 19).** To a 10-mm NMR tube at  $-78\text{ }^{\circ}\text{C}$  containing 3.7 mL of THF was added PhLi (0.25 mL, 0.158 mmol, 0.633 M in THF). The sample was titrated with HMPA at a probe temperature of  $-120\text{ }^{\circ}\text{C}$ . Referencing was by procedure A. The sample was quenched with 2 equiv of  $\text{Me}_2\text{S}_2$  (0.03 mL, 0.33 mmol). GC analysis of PhSMe gave an 88% recovery of PhLi for the reference sample which was titrated with up to 1.0 equiv of HMPA and a 49% recovery for the sample that had 10 equiv of HMPA added. Therefore, the PhLi shows some decomposition during the experiment at high HMPA concentrations.

**$^7\text{Li}$  and  $^{31}\text{P}$  NMR Spectroscopy of an HMPA Titration of MeLi in 3:2 THF/Ether (Figure 20).** A solution of MeLi (0.526 mL, 0.80 mmol, 1.52 M in ether), THF (2.40 mL), and ether (1.07 mL) was titrated with HMPA.  $^7\text{Li}$  and  $^{31}\text{P}$  spectra were taken at 0.125, 0.25, 0.375, 0.5, 0.625, 0.75, 1.0, 1.5, 2.0, 3.0, 4.0, and 6.0 equiv of HMPA. The probe temperature during the experiment was  $-135\text{ }^{\circ}\text{C}$ . Low-halide MeLi was purchased from Aldrich as a 1.4 M solution in ether (with a halide content of about 0.05 M or 3.6%, which was detectable by our NMR technique).

**Acknowledgment.** We gratefully acknowledge the financial support of the National Science Foundation for this work (CHE 8814876).